Automatically Measuring Neuromuscular Jitter

by

Xin Wang

A thesis
presented to the University of Waterloo
in fulfilment of the
thesis requirement for the degree of
Master of Applied Science
in
Systems Design Engineering

Waterloo, Ontario, Canada, 2005

© Xin Wang, 2005

I hereby declare that I am the sole author of this thesis. This is a true copy of the thesis, including any required final revisions, as accepted by my examiners.

I understand that my thesis may be made electronically available to the public.

Abstract

The analysis of electromyographic (EMG) signals detected during muscle contraction provides important information to aid in the diagnosis and characterization of neuromuscular disorders. One important analysis measures neuromuscular jitter, which is the variability of the time intervals between two muscle fibre potentials (MFPs) belonging to the same motor unit over a set of discharges. Conventionally, neuromuscular jitter is measured using single fibre (SF) EMG techniques, which can identify individual MFPs by using a SF needle electrode. However, SF electrodes are expensive, very sensitive to needle movement and not easy to operate in practise.

A method is studied in this thesis for automatically measuring neuromuscular jitter in motor unit potentials (MUP), it measures jitter using routine EMG techniques, which detect MUPs using a concentric needle (CN) electrode. The method is based on the detection of near MFP contributions, which correspond to individual muscle fibre contributions to MUPs, and the identification of individual MFP pairs. The method was evaluated using simulated EMG data. After an EMG signal is decomposed into MUP trains, a second-order differentiator, McGill filter, is applied to detect near MFP contributions to MUPs. Then, using nearest neighbour clustering and minimum spanning tree algorithms, the sets of available filtered MUPs can be selected and individual MFPs can be identified according to the features of their shapes. Finally, individual MFP pairs are selected and neuromuscular jitter is measured.

Using the McGill filter, near MFP contributions to detected CN MUPs can be consistently detected across an ensemble of successive firings of a motor unit. The method is an extension of the work Sheng Ma, compared to previous works, more efficient algorithms are used which have demonstrated acceptable performance, and which can consistently measure neuromuscular jitter in a variety of EMG signals.

Acknowledgements

I would like to express my sincere gratitude and appreciation to my supervisor Dr. Dan Stashuk. His continuous guidance, support and inspiration during my graduate study and my research made this work possible.

I would also like to thank my thesis readers, Dr. Gordon J. Savage and Dr. John S. Zelek for reviewing of this thesis and their helpful comments and suggestions.

I would like to thank my parents, Wenbo Wang and Fengzhen Li, my sister, Ying Wang for giving me their love, support and encouragement all the time.

Contents

List of Tables

List of Figures

Chapter1 Background knowledge of neuromuscular electrophysiology and EMG signals

1.1 Introduction

The study of electromyographic (EMG) signals is a study of the electrical properties and activities of muscle tissue. EMG signals are detected by placing an electrode into, or over a muscle and detecting the extracellular voltages produced by the electrical activity of the muscle fibres. In various types of examination, these signals will either be induced voluntarily by the patient, induced by stimulating the nerve supplying the muscle, or induced by moving the needle electrode. For this work, we restrict our interest to activity detected during voluntary contraction of a muscle by a patient attempting to keep the force of contraction as constant as possible.

The analysis of EMG signals detected during muscle contraction provides important information to aid in the diagnosis and characterization of neuromuscular disorders. Clinical electromyography is the study of the function of the neuromuscular system through the analysis of EMG signals. In general, the characteristics of EMG signals are dependent on a number of factors, including the anatomical and physiological properties of the related neuromuscular system, the level of muscle contraction, the type of electrode used and the location of the electrode relative to the contracting muscle fibres. Clinical electromyography developed into a useful technique for clinical examination after the introduction of the concentric needle electrode by Adrian and Bronk in 1929 [1].

Traditionally, the analysis of clinical EMG signals has been performed by human experts. This work requires a good deal of skill and experience, and is quite time-consuming. It relies heavily on the ability of an electromyographer to detect visually and acoustically specific characteristics of an EMG signal. The number of applications using computers and modern signal processing technologies for the analysis of EMG signals are growing rapidly. Presently, interest has been focused on the ability to analyze EMG signals automatically and quantitatively.

This chapter briefly describes neuromuscular physiology and the generation of EMG signals. Also, some basic concepts and characteristics of EMG signals are presented. The configurations of a few kinds of needle electrodes are briefly introduced.

1.2 Neuromuscular Physiology

Skeletal muscle is composed of a large number of individual parallel, cylindrical muscle cells, which are called muscle fibres. The muscle fibre is a multinucleated cell with a diameter from 10 to 100 micrometers (μm), and a length from a few millimeters to several centimeters (up to 30 cm) [1] (see Figure 1.1). Each muscle fiber contains myofibrils that are long slender arrays of contractile proteins that align along the length of the cell such that the cell appears striped. They are organized into a bundle by connective tissue, and are attached to the bones by tendons. When the muscle fibres are activated, the muscle contracts and generates force. EMG signals are acquired from skeletal muscle.

The tissues of both the muscular and nervous systems are composed of 'excitable cells'. All cells are surrounded by a cellular membrane, which controls the relative concentration of various species of ions inside and outside the cell body. The concentration of several ions is quite different on one side of the membrane than on the other. This results in an electrical charge difference. When the electrical signal from the nerve arrives at the muscle fibre, the fibre membrane is excited (called depolarization). An action potential is then generated and propagates along the membrane, and electrochemical interactions, which result in muscle fibre contraction, take place.

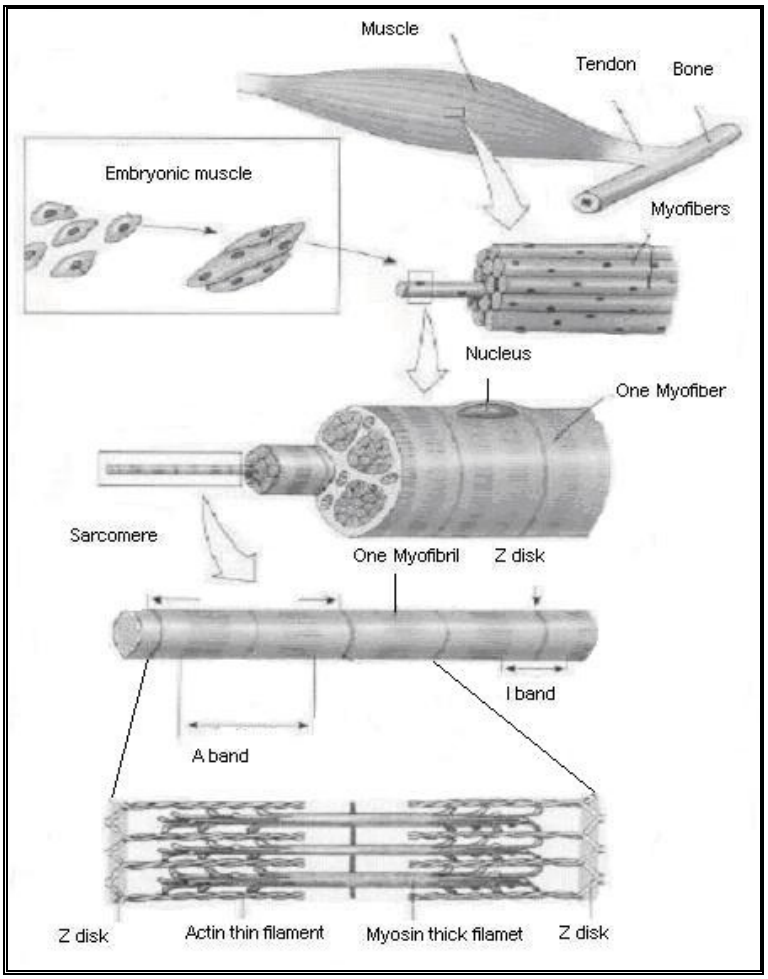

Figure 1.1: General Structure of skeleton muscle [33]

In normal skeletal muscle, fibres never contract by themselves. Instead, individual muscle fibres are organized into motor units, the fundamental functional units of the neuromuscular system. A motor unit consists of an alpha motoneuron and all the muscle fibres it innervates. The body of a motoneuron is located in the anterior horn of the spinal chord, and the motoneuron has an axon that extends all the way to the muscle fibres. Before it reaches the muscle fibres, it splits into many branches called axon terminals. These axon terminals terminate on the muscle fibres. The zone where the axon terminals and muscle fibres contact is called the *endplate* or *neuromuscular junction* (NMJ). There is normally only one junction per fibre, and it is usually located near the middle of the muscle fibre (see Figure 1.2) [1].

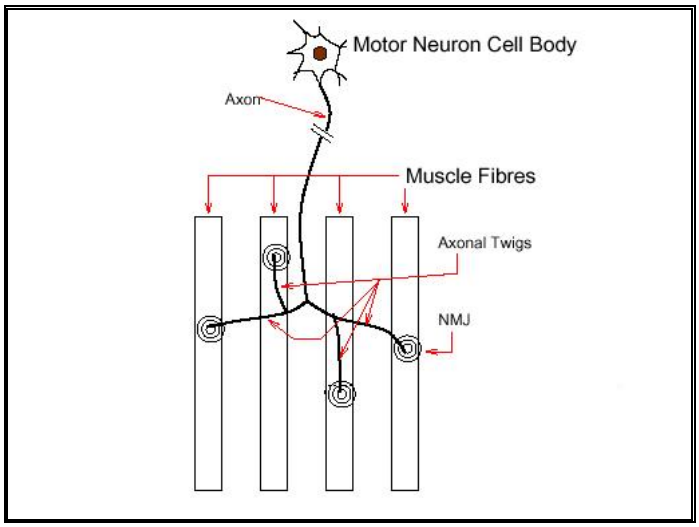

Figure 1.2: Diagram of a motor unit [1]

Each discharge of a motoneuron produces a propagating action potential. When the action potential reaches the NMJ, a new action potential is initiated in the muscle fibre membrane and the muscle fibre is activated. This action potential is then propagated over the excitable membrane of the muscle fibre in both directions towards the ends of the fibre and forms a potential field in the extracellular tissue around the muscle fibre. Therefore, *muscle fibre potentials* (MFPs) can be detected using a suitable electrode. The action potential propagating along a muscle fibre initiates its mechanical contraction. All fibres in one motor unit are activated at almost the same time but activity among different units is normally independent [2]. The superposition of the MFPs of all the fibres in a motor unit forms a *motor unit potential* (MUP). The repetitive discharge (firing) of a given motor unit creates a train of potentials known as a *motor unit potential train* (MUPT). An *electromyographic* (EMG) signal results from the detection of the electrical activity of all active motor units. In the following two sections the generation and characteristics of MFPs, MUPs, MUPTs and EMG signals will be discussed in more detail.

The sizes of motor units vary widely, and depend on both the number of muscle fibres in the unit and the diameter of individual fibres. A small motor unit may have fewer than 10 muscle fibres. This type of motor unit is responsible for very fine movements needed

for precise control, such as darting movements of the eyes. A large motor unit may have as many as several thousand muscle fibres. Such a motor unit is responsible for gross movements, such as contraction of the legs or the maintenance of posture [1]. The fibres of a specific motor unit are randomly distributed throughout a specific (approximately circular) muscle area, termed the motor unit territory (2-15 mm in diameter) [3]. The territories of a muscle's motor units are randomly distributed throughout the area of the muscle. Therefore, motor unit territories are intermingled or overlap, and muscle fibres belonging to one motor unit are not closely packed together, but are scattered over a small area of the muscle and intermingle with fibres belonging to other motor units (see figure 1.3). An area of 5-10 mm in diameter might contain muscle fibres from 15-30 motor units [3]. However, all of the muscle fibres in a motor unit are of the same biochemical and physiologic type (i.e., same twitch and fatigue characteristics), and are categorized according to their histochemical and contractile characteristics [1].

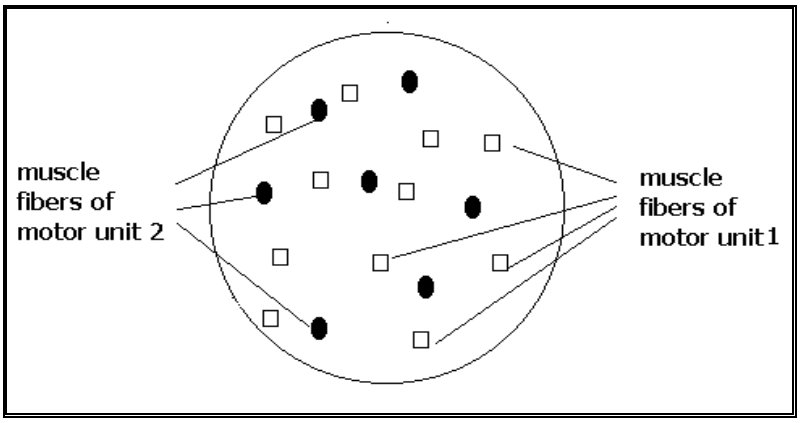

Figure 1.3: Cross-section of part of a muscle [4]

A motor unit can be electrically re-excited even if its fibres are not yet relaxed mechanically. The result of this phenomenon is to increase the force contributed by a motor unit to the total force produced by the muscle. The muscle force depends on two factors, the number of active motor units and the frequency of motor unit activation.

1.3 Muscle Fiber Potential (MFP)

As previously mentioned, motoneurons and muscle fibres are excitable cells, i.e., they have the ability to generate a propagating transmembrane action potential after they are activated. The action potential is an all-or-none response to a stimulus. It is a transient change in the voltage across the membrane, and is propagated by the excitable cell. Once initiated by a sufficient stimulus, action potentials propagate along nerve and muscle fibres without decrement. Local currents flowing from the depolarized region stimulate the adjacent inactive region so that the action potential is propagated.

In a neuromuscular system, each discharge of an alpha motoneuron produces a propagating action potential across its axonal membrane. The propagating action potential travels along the axon terminals, and reaches the endplates to initiate an action potential on the muscle fibre membrane at each endplate (i.e., the NMJ is the initiation point of a propagating action potential in a muscle fibre). The action potential then propagates along the muscle fibre membrane in both directions towards the two ends of the muscle fibre, and triggers the coordinated contraction of the muscle fibre.

The propagation of an action potential along the muscle fibre also creates an electric field in the vicinity of the muscle fibre. This electric field can be detected using suitable electrodes located in this field. The acquired voltage waveform is known as a MFP. A MFP is a fundamental component of a detected EMG signal. In fact, an EMG signal results from contributions of electrical activity from all of the active muscle fibres.

A MFP waveform is typically a triphasic voltage waveform [3]. When the action potential propagates along the fibre toward the detection electrode, the first phase is created. Following that, the second phase is formed as the action potential begins to propagate away from the electrode. The second phase is a reversal of the first one, and usually contains the main peak of the MFP waveform. It is relatively brief and smooth. The third phase is a decaying phase after the second as the action potential continues to move away from the electrode, and is a reversal of the second phase (see Figure 1.4).

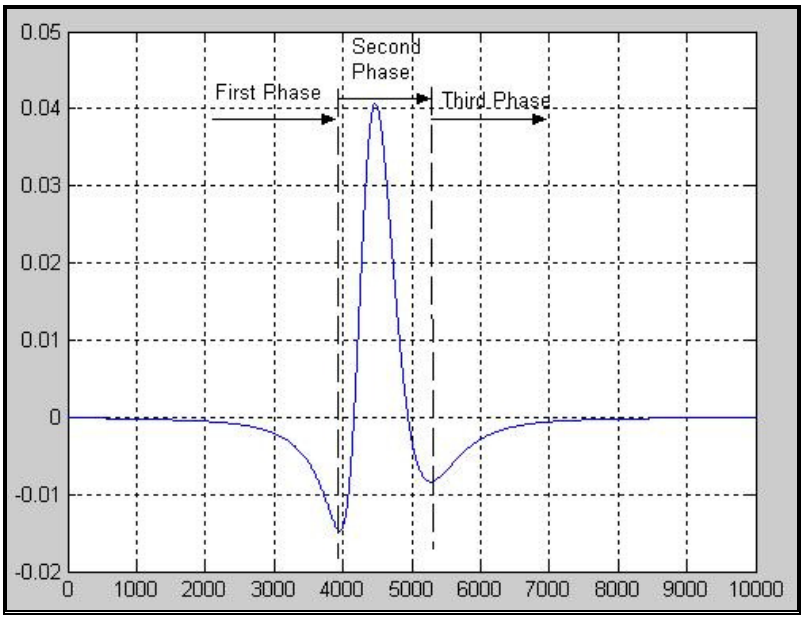

Figure 1.4: Typical MFP waveform

The shape and amplitude of a MFP are associated with muscle physiological properties and detection electrode characteristics. The duration of a MFP usually ranges from 2 to 6ms [3]. The waveform characteristics of the MFP depend on the diameter and length of the muscle fibre, the speed with which it conducts action potentials (i.e., the fibre's conduction velocity), the distance between the active muscle fibre and the detection site, and the configuration of the detection electrodes [6]. Larger diameter fibres create larger MFP amplitudes.

Slower conduction velocity and longer fibre length result in longer duration MFPs. The location of the detection site relative to the muscle fibre and its NMJ determine the maximum amplitude and initial value of the MFP, respectively. The magnitude and high frequency content of a MFP decrease as the distance between the fibre and the detection surface of the electrode increases (see Figure 1.5 (a) (b)). The peak-to-peak amplitude decreases by approximately 75% if the electrode is moved 100 μm from the surface of a fibre [6]. The magnitude also decreases as the detection area of the electrode increases [2] (see Figure 1.6).

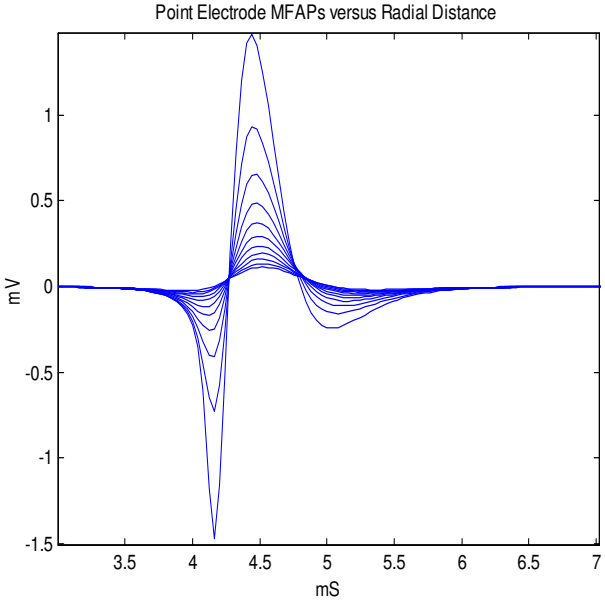

(a)

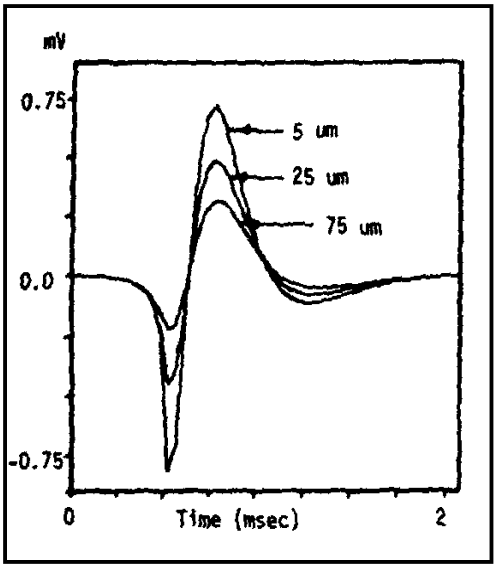

(b)

Figure 1.5: The effect of distance on the amplitude and the frequency content.
(a): Amplitude and frequency content versus distance [1]. (b): MFP size versus distance [6].

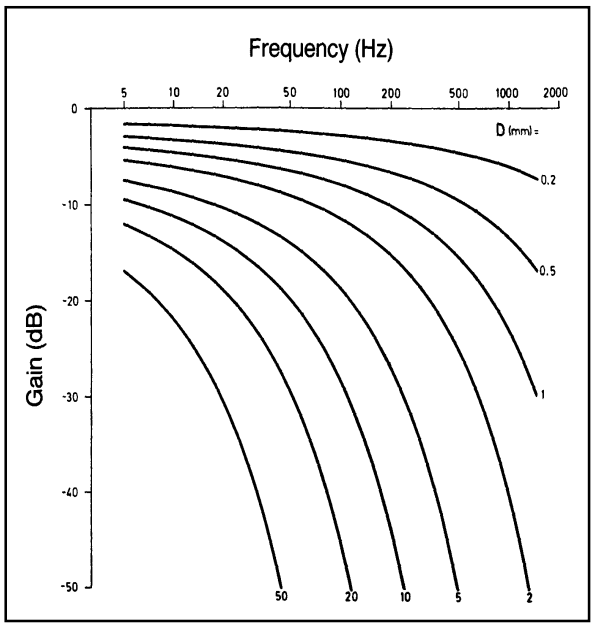

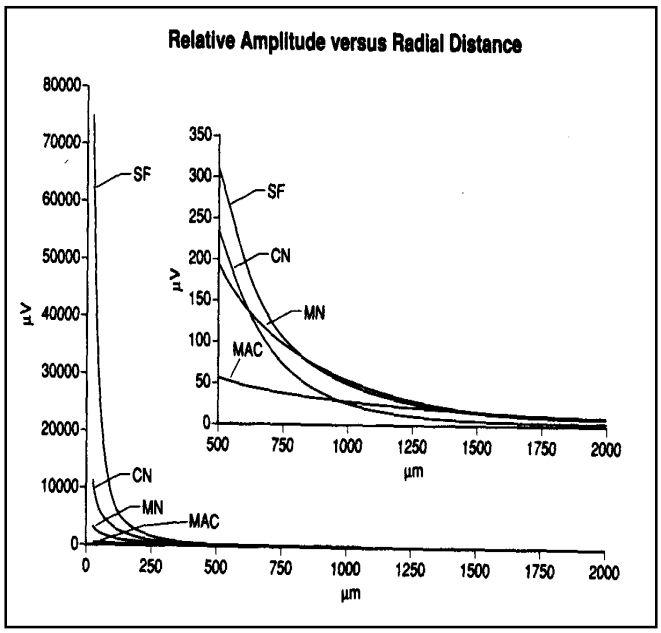

Figure 1.6: Amplitude versus electrode type and distance [7]

(SF = single fibre, CN = concentric, MN = monopolar needle, MAC = macro)

1.4 MUP Train and EMG Signal

The excitation of a muscle fibre is not isolated, and is controlled by the motor unit. During muscle contraction, all the fibres in a motor unit discharge roughly at the same time. For conventional clinical detection, MUPs are usually recorded by using the CN (Concentric Needle) electrode. A MUP is created by the summation of the spatially and temporally dispersed action potentials of the individual muscle fibres of the motor unit [1] (i.e. a MUP is the linear superposition of the individual MFPs of the fibres of the motor unit). Figure 1.7 represents the generation of a MUP.

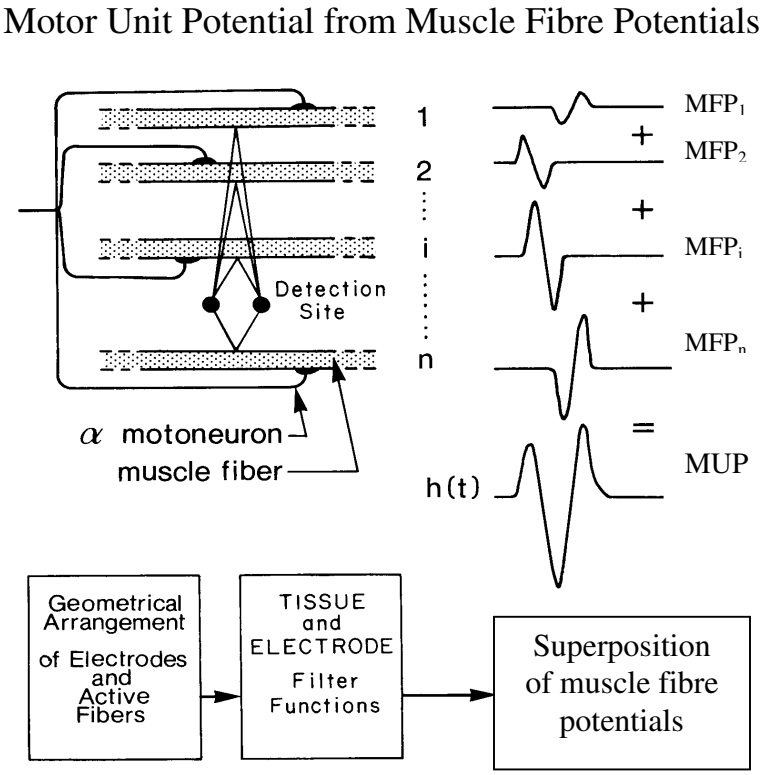

Figure 1.7: Schematic representation of the generation of a MUP [1]

The MUP can be expressed in a quantitative way [10]:

$$MUP_j(t) = \sum_{i=1}^{N_j} MFP_{ij}(t - \tau_i)s_i$$

where:

$MUP_j(t)$ is the voltage waveform detected when the j^{th} motor unit fires;
$MFP_{ij}(t)$ is the detected waveform resulting from an action potential propagating along the i^{th} fiber belonging to the j^{th} motor unit;
N_j is the number of fibers belonging to the j^{th} motor unit;
t expresses the certain detection moment;
τ_i is the temporal delay of $MFP_{ij}(t)$ at the detection site;
s_i is a random binary variable.

Each s_i value can be randomly selected for each firing of each motor unit, and represent neuromuscular junction function that has a value of 1 if the i^{th} fiber fires and 0 if the i^{th} fiber is blocked (i.e. does not fire).

τ_i represents the conduction delay. It is the temporal offset, and is associated with the location of the NMJ and the conduction velocity of the muscle fibre [10]. Its value fluctuates with each MU discharge. In normal muscle, assuming a constant detection configuration, the waveforms of the MUPs are usually quite constant across multiple MU discharges. Therefore, MUP shape information can be used to identify the MUPs created by the same motor unit. However, biological abnormality can cause variability of MUP shape. If the delays of the MFPs vary (τ_i changed with each MU discharge), the MUP waveforms will vary. In addition, possible changes in the position of the electrode relative to the muscle fibres (MFP_i changed) and the possibility of a particular fibre failing to fire (block; $s_i = 0$) can also cause stochastic biological variability of a MUP waveform. Although the number of fibres within a motor unit (N_j) can theoretically determine the size of the MUP, the size of the MUP is often dependent on the location and diameter of the closet few fibres because MFP size decreases as the distance to the detection electrode increases [11].

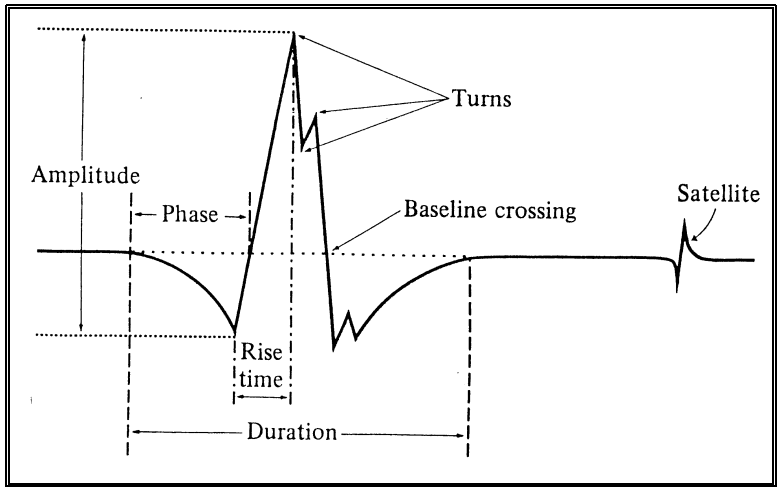

Figure 1.8: Definition of MUP features [11]

The waveform of most MUPs consists of at least three sub-components, which are an initial component, a main spike and a terminal component. It may also contain satellite potentials in some pathological MUPs. Features of a MUP can be described by the amplitude, rise time, duration, number of turns and phases (see Figure 1.8). Other morphological features include MUP variability and fibre density, etc. [11]. MUP variability is characterized by jitter and jiggle [12]. In the following chapter, jitter will be described in detail.

Individual MUPs can be isolated only during weak muscle contractions when one or a few motor units are active. During strong contractions, the MUPs activited are so numerous that the EMG signal acquired becomes a noise-like "interference pattern" [3].

The repetitive firing of a motor unit produces a sequence of MUPs. The collection of MUPs generated by one motor unit is known as a *motor unit potential train* (MUPT). Motor units repeatedly discharge (fire) in order to maintain or increase the force output of a muscle. The time interval between successive discharges is called an inter-discharge interval (IDI). In a MUPT, MUPs are positioned and separated by their IDIs. The discharges of a motor unit are repetitive but not periodic. The variation range of IDIs is normally from 20 to 200ms [2]. A MUPT can be is mathematically expressed as [30]:

$$MUPT_k(t) = \sum_{i=1}^{N_k} MUP_{ik}(t - \delta_{ki})$$

where:

$MUPT_k(t)$ is the MUPT of the k^{th} motor unit;
$MUP_{ik}(t)$ is the MUP generated during the i^{th} firing of the k^{th} motor unit;
N_k is the number of times the k^{th} motor unit fires;and
δ_{ki} is the i^{th} firing time of the k^{th} motor unit.

If the occurrence times of MUPs in a MUPT are marked by delta impulses and the MUPs are represented by a filter whose impulse response is *h(t)*, then the impulses are passed through the filter and the output will be the MUPT. Like this, the MUPT can be modeled as a sequence of delta impulses [1] (see Figure 1.9).

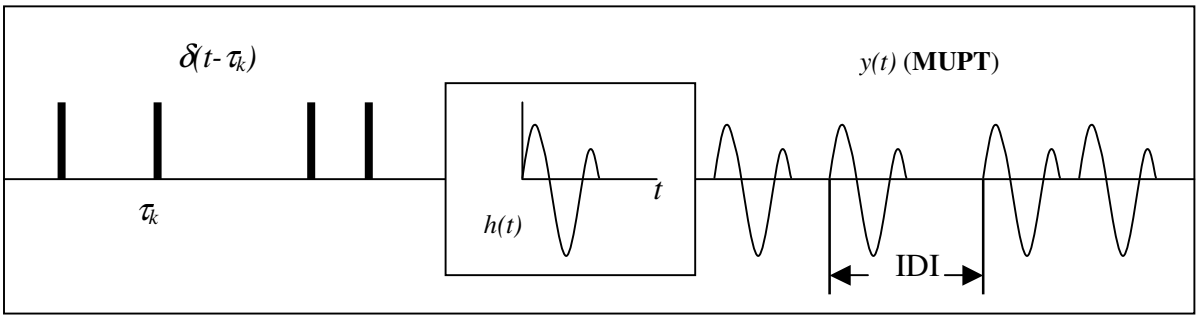

Figure 1.9: Model for a motor unit potential train [1]

During the voluntary contraction of a muscle, the superposition of the MUPTs of all active motor units results in a composite EMG signal. It is the spatial and temporal sum of potential contributions from all excited muscle fibres. So, the composite EMG signal can be expressed by the summation of MUPTs of all recruited motor units.

$$EMG(t) = \sum_{m=1}^{N_m} MUPT_m(t) + n(t)$$

where:

$MUPT_m(t)$ is the m^{th} MUPT;
N_m is the number of active motor units;
n(t) is the background instrumentation noise.

Figure 1.10 represents the physiological and mathematical model for the composition of a detected EMG signal. The actual composition of an EMG signal is associated with the detection site and the configuration of the electrode. Using an electrode with a very small detection surface, such as a SF electrode, EMG signals may primarily be the record of the electrical activity of only one or a few of the closet fibres. Clinically, however, EMG signals are usually detected using a CN electrode, and consist of the electrical activity of many fibres from various motor units.

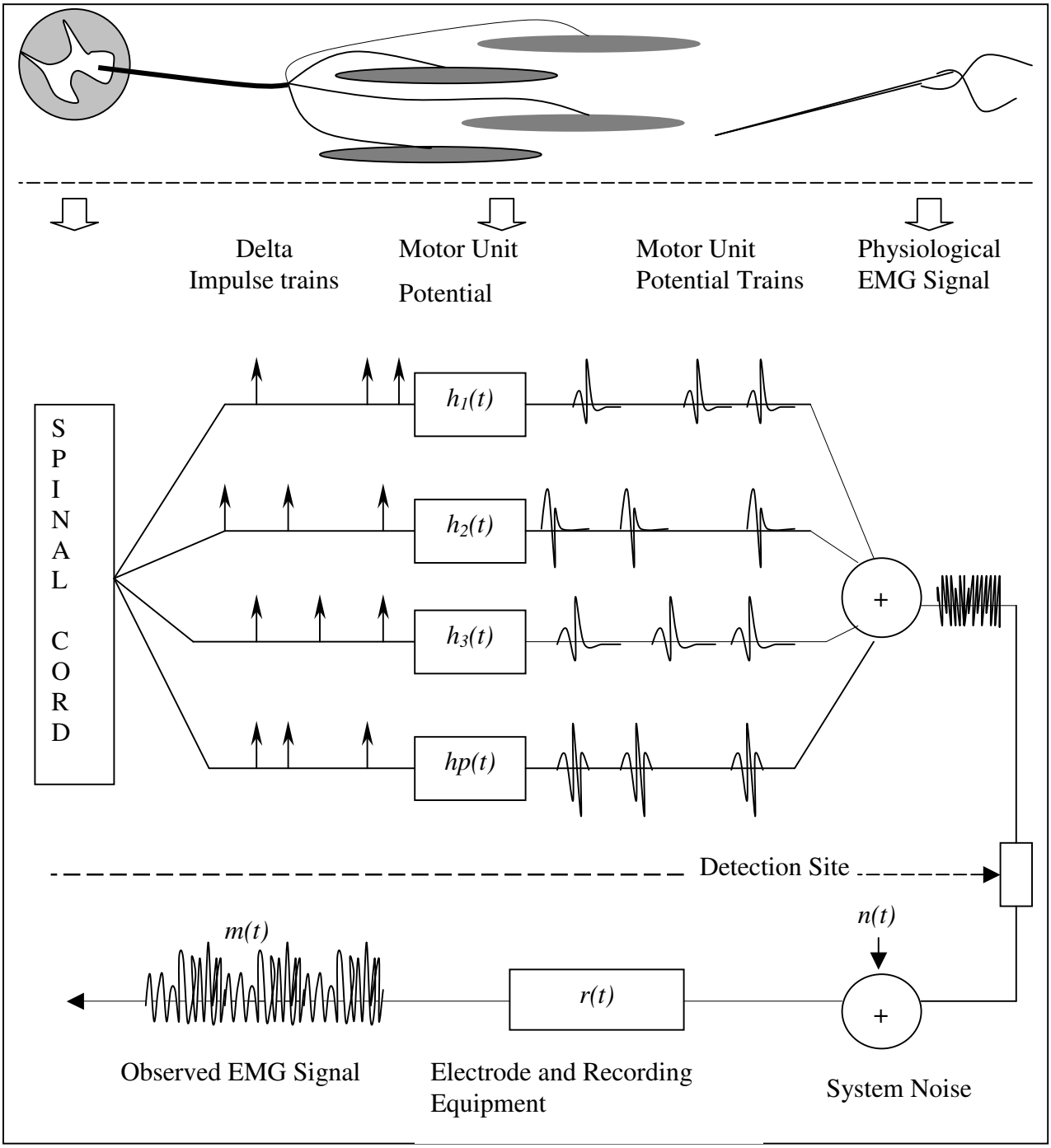

Figure 1.10: Model for the composition of an EMG signal [1]

1.5 Needle Electrodes

Depending on the various kinds of electrodes, the acquired EMG signals can be classified into micro signals and macro signals. Micro signals are detected by using indwelling electrodes which have small, selective detection surfaces, such as single fibre (SF) needle electrodes, concentric needle (CN) electrodes, monopolar needle (MN) electrodes and fine-wire electrodes. Micro signals can describe the electrical activity of individual motor units. Macro signals are acquired by using surface or indwelling macro or conmac electrodes. Macro signals are usually used to detect EMG signals over a large spatial extent, and may help determine the size of the motor unit [6]. This thesis only deals with micro signals acquired by needle electrodes. The characteristics of the three kinds of needle electrodes can be described as follows.

The SF electrode is a specially constructed needle electrode for recording SF EMG signals. It is highly selective and primarily reflects the activities of only those muscle fibres within the immediate vicinity of the detection surface. Therefore, it can selectively detect potentials produced by individual muscle fibres. The selectivity results from the small leading-off detection surface, 25 μm in diameter, which is exposed at a port on the side of the needle cannula located 7.5 mm from the tip [6]. When the SF electrode is randomly inserted in the muscle, it usually primarily records the electrical activity of one (in 70%) or sometimes two muscle fibres (about 25%) belonging to the same motor unit at one detection site [13].

The main spike of the single MFP is relatively brief (See Figure 1.5). It has a shorter duration (mean: 0.470ms; range: 0.265 to 0.8 ms), faster rise time (often less than 0.150 ms; range: 0.067 to 0.200 ms), and considerably higher amplitude than those detected using conventional CN electrodes [3]. For example, the mean amplitude of a single MFP is 5.6 mV, and range from 0.7 to 25.2 mV [3].

CN electrodes were the first to be introduced and are the most commonly used in routine EMG examination. A CN electrode consists of an outer needle cannula and a central wire called the core. The core is insulated from the outer cannula. The tip of the CN electrode

needle is ground to an angle of 15°, exposing an elliptical detection surface of the core, with a major axis of 580 μm and a minor axis of 150 μm with an area of 0.07 mm^2 [6]. The outer diameter of the cannula is 0.45-0.55mm, and is used as the reference electrode. The difference between the potentials detected by the core and the cannula is the CN MUP.

The primary advantage of CN electrodes is that they are remarkably durable, disposable and widely used. Observations made with them are very reproducible. MUPs recorded during minimal voluntary contraction with CN electrodes primarily represent the summated electrical activity of all muscle fibres in the active motor units within approximately 1 mm of the electrode tip. The steep decline in the peak-to-peak amplitude of the detected potentials with distance from the electrode means that only those muscle fibres within approximately 0.5 mm of the electrode make significant contributions to the detected MUPs. Because the width of most motor unit territories can be as wide as 5 to 10 mm or more, the majority of muscle fibres belonging to a motor unit may make very little contribution to the peak-to-peak amplitude of the MUPs due to their relatively large distance from the electrode [3]. Actually, the spike components of the CN MUPs (acquired by a CN electrode) are produced predominantly by the closest 2-12 muscle fibres [14].

MN electrodes are made from stainless steel wire (0.3 to 0.5 mm in diameter) sharpened at the tip. The electrode is insulated except at the tip, the bare tip extending back 25 to 50μm or more. The exposed conical detection surface area of MN electrodes is approximately 0.24 mm^2. A surface or subcutaneous electrode is often used to serve as the reference [3].

One of the advantages of MN electrodes is their larger detection area that may result in the detection of larger MUPs because the electrode is closer to a larger number of fibres from the same motor unit. However, temporal overlap of MUPs detected using MN electrodes occurs more frequently than when using CN or SF electrodes.

In most muscle, the duration of MUPs detected by CN or MN electrodes are several times longer than the duration of individual MFPs [3]. The duration also depends on the

bandwidth of the recording system. Most electrodes that are used in detecting EMG signals may be usually considered to be a high-pass filter. The characteristics of the high-pass filter can attenuate the MFP contributions of more distant fibres in relation to the contributions of the muscle fibres in the immediate vicinity of the electrode. This reduces the effective detection area of the electrode and makes the electrode more useful for detecting the electrical activity of individual fibres [1]. The comparison of the effective detection areas of SF, CN and MN electrodes are illustrated in Figure 1.11.

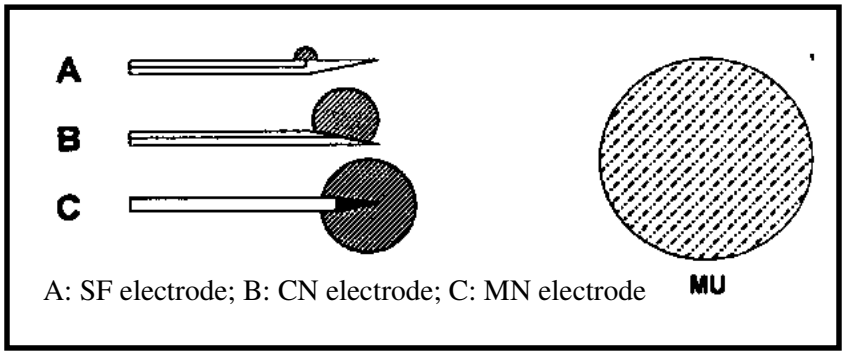

Figure 1.11: Comparison of the detection areas of a SF, CN and MN electrode [6]

With respect to detected MUPs, the relative properties of the SF, CN and MN electrode have been studied. For the MN electrode with a maximum 90% sensitivity of the amplitude, (i.e. the distance at which the amplitudes of MFPs fall to 10% of the maximum recorded at the detection surface.) the recording radius is approximately 425 μm, and encompasses approximately 60 fibres. The 90% sensitivity radius for a CN electrode is 280 μm and encompasses about 12 fibres. The 90% sensitivity radius for SF electrode is 110 μm and encompasses only 1-3 fibres. In addition, the radii of the 99% amplitude sensitivity are 1900 μm for a MN electrode, 830 μm for a CN electrode and 320 μm for a SF electrode, respectively (see Figure 1.12) [7].

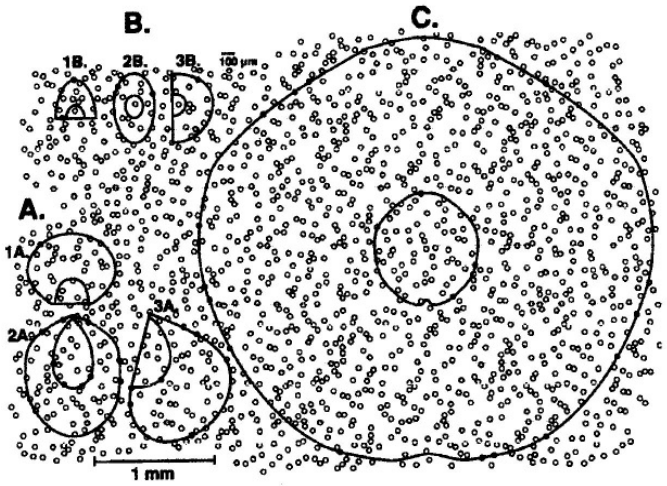

Figure 1.12: Comparison of 90% (inside circle) and 99% (outside circle) sensitivity isopotentials for CN, MN and SF electrodes. (A): CN electrode (1A: top; 2A: front; 3A: side views). (B): SF electrode (1B: top; 2B: front; 3B: side views). (C): MN electrode (side view). Muscle fibres from a single motor unit are 50 µm in diameter and their distribution pattern has been duplicated several times for illustration purposes. [7]

The MUPs detected with a CN electrode during slight voluntary muscle contraction are usually primarily generated by several muscle fibres. These MUPs can be considered as the composite potential of several individual MFPs. These MFP contributions are primarily of relatively high frequency content and are created by the relatively few fibres closest to the electrode. The shapes of the MUPs are also determined by the occurrence time of the MFPs due to the different locations of the NMJs and the different propagation velocities of the different muscle fibres [10]. Consequently, CN MUP waveforms have more turns, phases, amplitude changes, and are more complicated than SF MUP (acquired by using a SF electrode) waveforms (see Figure 1.13). It is also harder to isolate individual MFP contributions from these CN MUPs.

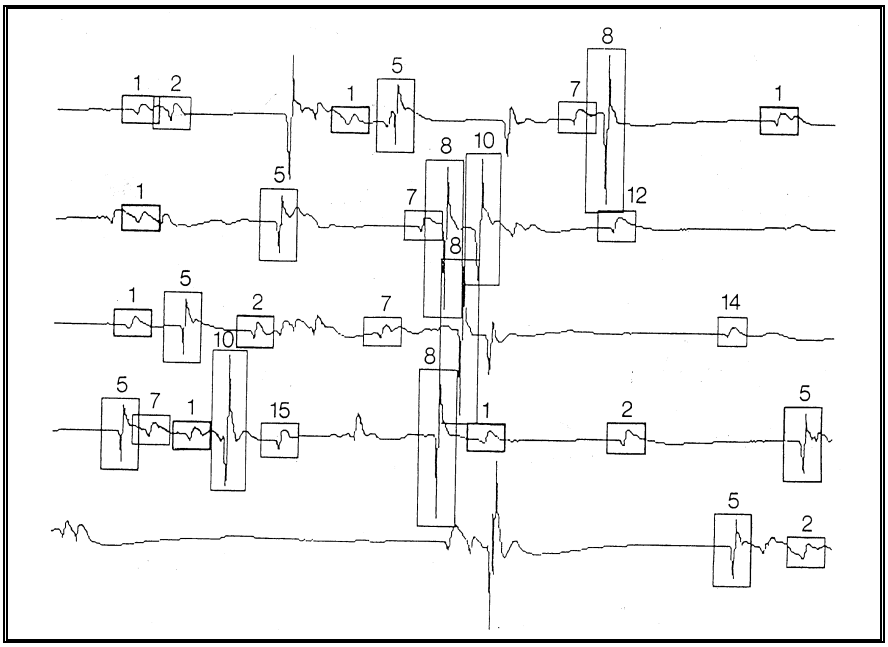

Figure 1.14: Various shapes of CN MUPs

Since its introduction, the CN electrode has found wide application in the clinical diagnosis of neuromuscular diseases. It can usually provide a reasonable balance of sensitivity and selectivity for detecting MUPs, and it is convenient to use [7]. The MN electrode is less convenient for the examiner because of the need for a separate surface reference electrode. In addition, due to the larger conical detection surface, the MUPs detected by MN electrodes have greater amplitude and complexity (larger number of phases and turns) compared to MUPs detected by CN electrodes. However, there is no significant difference in mean MUP durations [14].

1.6 The Decomposition of EMG Signals

The shape, size, complexity and stability of MUPs can provide information related to the morphology and physiology of the motor unit. In the practical setting, the raw signals acquired by detection electrodes are always composite EMG signals. To assess functions

of a neuromuscular system, some characteristics of MUP waveforms have to be measured in a quantitative way in order to get a more faithful representation of the events occurring within the muscle. Therefore, composite EMG signals have to be decomposed into isolated MUPs of individual motor units. Decomposition of the EMG signal is the procedure by which an EMG signal is separated into its constituent MUPTs .

An automated decomposition and quantitative EMG signal analysis system (DQEMG) has been developed at the University of Waterloo. The DQEMG system consists of signal acquisition, MUP detection, MUP clustering and supervised classification, and estimation of MUP templates as well as the measurement and analysis of MUP parameters.

During signal acquisition, an acquired EMG signal is amplified and filtered. The signal is then digitized, and sampled at a rate of 31.25 kHz. After MUP detection, clustering and supervised classification, the raw EMG signal has been decomposed into the isolated MUPs and MUPTs. MUP templates for every MUPT are then estimated. Finally, characteristic parameters, such as duration, amplitude, rise-time, number of phases and number of turns, etc., are measured for each MUP template, and motor unit firing behaviour is analyzed. In addition, other morphological features, such as fibre density, neuromuscular jitter and jiggle, are also tentatively measured. The first step of automated jitter measurement will be based on the result of EMG signal decomposition, this will be further discussed in Charpter 2.

Chapter 2 Neuromuscular Jitter and Measurement

2.1 Overview

Jitter is a measurement of the variation of the time intervals between pairs of MFP contributions to MUPs. The jitter phenomenon was originally studied by Ekstedt (1964) using SF EMG signals[17]. The measurement and analysis of the jitter is especially useful for evaluation of neuromuscular junction dysfunction. It is a sensitive clinical test for detecting a mild defect of neuromuscular transmission [17]. The individual action potentials of the different muscle fibres of a MU are separated in time from each other because of different NMJ delays and propagation velocities along different nerve branches and muscle fibres. However, the conduction velocities for individual muscle fibres and nerve branches are relatively fixed. Therefore, the time separation variations of MFP contributions mainly result from the random process of AcH released at each individual neuromuscular junction [16]. This random process makes the time of initiation of every individual MFP a random variable, and leads to the variable time intervals between the MFPs of a MUP. The variability of the time intervals between two MFPs generated by two muscle fibres of the same motor unit is referred to as neuromuscular jitter [25].

Traditionally, the jitter measurement has been implemented using SF MUPs detected using SF electrodes, which are primarily composed of contributions from one or just a few MFPs. However, SF electrodes are expensive, and very sensitive to needle movement. Therefore, it is necessary for physicians to have good dexterity and for subjects to cooperate in order to obtain useful SF EMG data. It would be advantageous if jitter could be measured using more economical and convenient CN electrodes [18], which is the major topic of this thesis.

This chapter describes the origin and influencing factors of neuromuscular jitter. It also presents the traditional methods of jitter measurement and calculation. In the last section, the concept of near individual MFP contributions is introduced.

2.2 Neuromuscular Jitter and Factors that Affect Jitter

Jitter is due to variable transmission times at the NMJ and, to a minor degree, variation in action potential propagation velocities along nerve and muscle fibres [17]. Therefore, neuromuscular jitter is primarily a measurement of the variability of NMJ transmission time. When two muscle fibres from the same motor unit are sufficiently close to an electrode detection surface that significant potentials can be detected from each of them, an individual MFP pair can be obtained. However, if the two potentials are so simultaneous in their time of initiation as to interfere with each other, a composite potential will be produced such that the individual MFP pair cannot be detected. Only when the two MFPs are sufficiently separated in time so as not to interfere with each other, can a potential pair can be detected. Such a potential pair will always occur together at consecutive MU discharges. If the occurrence of the first potential of the pair is used as a time reference, the second potential in the pair for each discharge occurs at a somewhat different time interval. The time interval between the two potentials of a pair is the inter-potential interval (IPI) (see Figure 2.1). The variability of the IPIs is the jitter.

The IPI depends on the difference in propagation times of the action potentials from the nerve branches to the detection site of the electrode. A motorneuron axon splits into axon terminals, and ends at the NMJs of the two muscle fibres (See Figure 2.1). Close to the branching point the nerve action potentials of the two axon terminals are simultaneous, but the propagation velocities in the two axon terminals or the length of the two axon terminals may be different; the synaptic delay of the two NMJs may be also different; the distances between the NMJs on the two muscle fibres and the detection site of the electrode may be unequal; the conduction velocity of the two muscle fibres may be also different. The combination of all these factors results in the IPI. The variability of the IPIs across a number of MU firings results in neuromuscular jitter.

Normally IPIs vary only slightly from one MU discharge to the next. Jitter is increased in neuromuscular disorders, such as myasthenia gravis that impairs NMJ transmission. In cases of severe disturbance of NMJ transmission, individual MFPs may occasionally be missing. This phenomenon is denoted as blocking. Particularly, as jitter increases, blocking of one or more potentials will occur, and indicates failure of NMJ

transmission [33]. For abnormal neuromuscular jitter, some researches have shown that variability in the propagation velocity in both the axon terminals and the muscle fibres is probably not an important factor; the difference in length of the axon terminals and the muscle fibres is also not an important contribution to jitter. Ekstedt [7] considered that the variability in the synaptic delay of the NMJs was the most important factor. For example, an increase of the jitter can be obtained by injection of D-tubocurarine, which only affects NMJ transmission. However, disease and pathological changes in the axon terminals or muscle fibres (such as muscular ischemia and dystrophy) may also cause increased jitter [17].

Change of temperature can also affect the jitter. Jitter increases when the muscle temperature is lowered and decreases slightly at warming. Nonetheless, slight muscle activity does not influence the jitter in a normal muscle. In addition, firing rate has only a little or no effect on jitter in a normal NMJ. For an abnormal NMJ, the firing rate has a variable effect on jitter. Furthermore, there is a significant difference in the mean jitter values in different muscles [24].

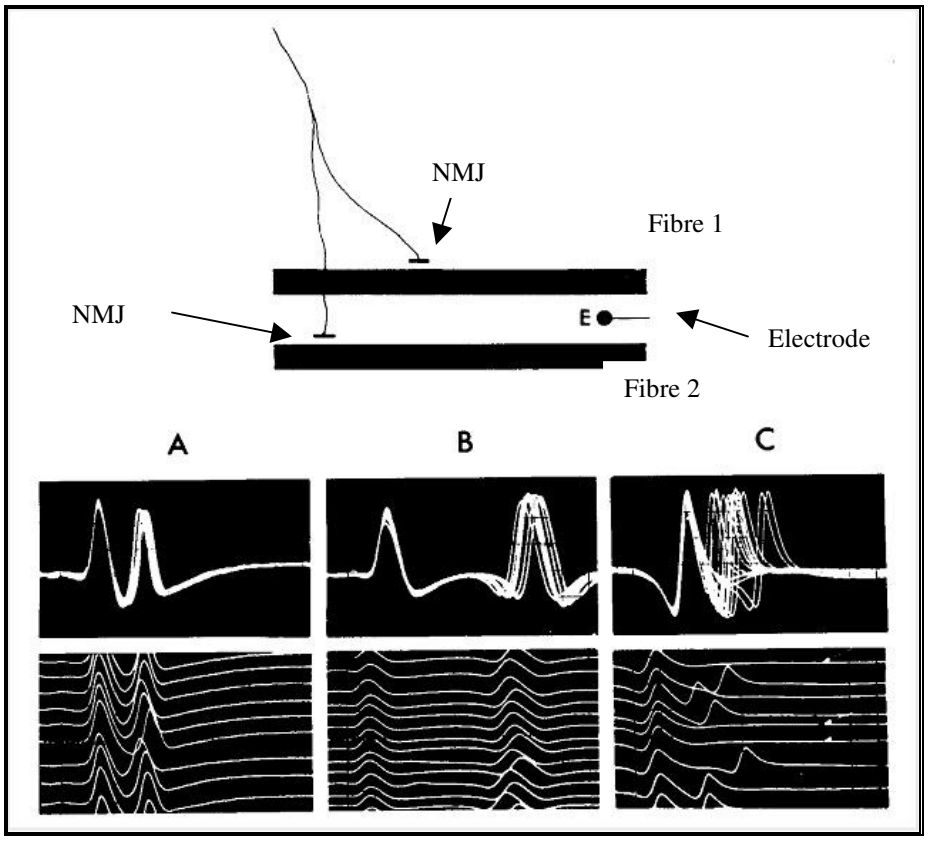

Figure 2.1: Schematic representation of jitter detection, two muscle fibres and electrode. A, B and C show MFP pairs raster with increasing jitter value, with the first MFP being time reference, we can get jitter from the time variability of second MFP. [2]

2.3 Traditional Methods for Measuring Jitter

Traditionally SF EMG data are used to measure neuromuscular jitter. SF EMG signals can be acquired using SF electrodes. Because the size of the detection surface of a SF electrode is small , it can be considered a single detection point. The amplitude of signals detected by this surface falls off rapidly as the distance between the electrode and the signal source increases. Therefore, the significant high frequency energy content of the signals is mainly contributed by a small number of fibres located close to the detection

surface of the SF electrode. In addition, using a high-pass filter with a 500 Hz low-pass cut-off frequency can further increase the selectivity of the detection because MFPs from distant fibres usually contain relatively more low-frequency components than MFPs from fibres closer to the electrode detection surface [19]. Therefore, the MUPs detected using a SF electrode should be individual MFPs, which can be verified by the shape of the MUPs. If peak components of detected MUPs have a stable shape and no bifurcation across an ensemble of repeated discharges of the motor unit, these peaks can be considered as representing individual MFPs (i.e., created by single fibre contributions).

Detection of individual MFPs requires that the subject maintains a minimal level of muscle contraction so that the electrode does not move during detection. The muscle contraction can be created in two ways: voluntary contraction and electrical stimulation.

Usually, SF EMG data collected during slight voluntary contraction of the muscle are used for measuring neuromuscular jitter. During voluntary contraction, the electrode is inserted into the muscle near the NMJ zone and positioned to detect two or more stable and clear individual MFP peaks from the same motor unit. The electrode position can be slightly adjusted in order to obtain the best detection site, where each potential peak to be used for the jitter measurement has a sharp rising phase and adequate amplitude. However, it is not necessary to position the electrode for maximum amplitude. In fact, at most sites within a muscle, the SF electrode is usually positioned so that detected MUPs have amplitudes greater than 200 μV and rise times less than 300μs, since potentials greater than 200 μV arise from muscle fibres within 300 μm of the detection surface. Clear individual MFPs detected using a SF electrode should be smooth, biphasic or triphasic and stable across a set of MU discharges [16]. A constant detection position has to be maintained while at least 50 discharges are collected. The IPIs are often measured between the baseline intersections of the steep positive-negative deflections of the MFP pairs. In addition, jitter should be detected from 20 different MFP pairs [20]. The time resolution of the detection system should be 10 μs or better [21].

Electrical stimulation techniques can be used for subjects who have difficulty maintaining constant voluntary contraction of the muscle. The stimulation is delivered at 2-10 Hz, where 10 Hz is usually used to approximate physiologic activation rates. The

stimulation intensity is adjusted to produce a slight twitch of the muscle. The electrode is inserted into the twitching portion of the muscle and positioned to detect clearly defined individual MFPs. The jitter measured between the stimuli and individual MFPs when further increasing the stimulation intensity does not decrease the measured jitter [20].

Individual MFPs elicited by nerve stimulation have jitter greater than MFPs elicited by direct muscle fibre stimulation. Some jitter may be introduced by variations in the intensity of the stimulus that reaches the individual motorneuron, especially when surface stimulation is used. Expertise is required to avoid misinterpretation when increased jitter is seen during axonal stimulation. The advantages of the electrical stimulation include perfect control of discharge rate and little need for subject cooperation. The additional discomfort of electrical stimulation is minimal and compared to voluntary contraction it may be preferred by some subjects [22].

In comparison to other EMG techniques MUPs detected using a SF electrode have less interference from adjacent fibres of other MUs during slight voluntary contraction. The SF EMG technique is the most sensitive electrophysiological method for diagnosing myasthenia gravis by measuring neuromuscular jitter. It can be of great value in demonstrating or excluding abnormalities in patients with mild or questionable muscle and neuronal diseases that are not apparent by other EMG techniques. SF EMG is also utilized in the investigation of a gamut of neuromuscular disorders as well as in the measurement of fibre propagation velocity and muscle fibre density.

2.4 Jitter Calculation Methods and Reference Values

2.4.1 Calculation Methods

Jitter is a measurement of the variation of the time intervals between pairs of MFP contributions to MUPs. The most common way of expressing variability is to use standard deviation (SD). The IPIs, however, may slowly increase or decrease because of electrode movement, or changes in action potential propagation velocities, or other

factors. If the variation is expressed as the standard deviation of a series of intervals, the SD may not be an accurate measure of jitter in this case. To minimize the influence of such slow variations, the jitter is expressed as the mean value of consecutive differences (MCD) of successive IPIs by the following formula [23]:

$$MCD = \frac{|IPI_1 - IPI_2| + |IPI_2 - IPI_3| + ... + |IPI_{n-1} - IPI_n|}{n-1}$$

where:

IPI_i is the i^{th} inter-potential interval, or the stimulus-response interval when stimulation is used.

MCD has the advantage of being more easily calculated than the standard deviation. In normal individuals, the jitter values are about 25 μs [24].

In certain situations, the IPI may be influenced by the preceding inter-discharge interval (IDI), which may introduce an additional variation due to changes in the velocity of action potential propagation alongin the muscle fibres [20]. When jitter is measured during voluntary contraction, the effect of variable firing rates can be minimized by sorting the IPIs according to the length of the preceding IDI, and then calculating the mean of the consecutive IPI differences in the new sequence. The result is called the mean of sorted-data difference (MSD). If the ratio of MCD/MSD is greater than 1.25, then the variations in the firing rate have contributed to the jitter, and the jitter value should be represented by MSD. Otherwise, MCD is used to express the jitter value, i.e.,

If MCD : MSD <= 1.25, Jitter value = MCD;

If MCD : MSD > 1.25, Jitter value = MSD;

It is suggested that jitter values that are greater than 150 μs should be excluded in order to avoid a few individual jitter values affecting the mean MCD value [23]. Jitter measurement summaries should include:

i. The mean or median value of the MCD value (In normal muscle, the mean and median MCD values are the same.);

ii. The percentage of the blocking;and

iii. The percentage of the abnormal pairs or NMJs.

During axonal stimulation, the MCD value measured is less than that measured during voluntary contraction of the same muscle because the jitter measured during axonal stimulation comes from only a single NMJ. In this case, the mean MCD value should be expressed by the following formula [20]:

Mean MCD (axonal stimulation) = Mean MCD (voluntary activation) / $\sqrt{2}$

In the calculation of jitter, the operator may select the interesting signal segments and exclude undesired signals according to the quality of the acquired signals. For each jitter analysis, 50 to 100 consecutive discharges should be recorded for each MFP pair. The jitter values of at least 20 different MFP pairs should be calculated for each subject [20].

In addition, there may be some variation in the jitter measured by different operators using different equipment. There are greater differences across different operators using the same equipment than across the same operator using different equipment. Selection of the detection position of the electrode and the epoch to analyze has more effect on the jitter results than does the equipment [20].

2.4.2 Reference Values

Normal jitter values vary with different NMJs in a muscle, with different muscles and with age, ranging from 10 to 50 μs [24]. With increased age, there is a slight increase in jitter in normal subjects. In addition, the IPI should be smaller than 4 ms and greater than 150 μs [24]. For long IPI values, particularly if the firing rate is irregular, the MSD calculation method does not completely compensate for the effects of action potential propagation velocity variations so that erroneously high jitter values may be obtained [20].

A jitter value of 5 μs or less is rarely obtained in SF EMG signals acquired by voluntary contraction in normal muscles and is more often measured in myopathic muscle. MCD values of 4 μs or less obtained during stimulation SF EMG indicate that the muscle fibre is being directly stimulated; these values should not be used for assessment of neuromuscular transmission [20].

The jitter is abnormal if either of the following criteria is met [20]:

i. The mean (or median) jitter exceeds the upper limit for the muscle.

ii. More than 10% of the pairs or NMJs have increased jitter.

2.5 Detecting Neuromuscular Jitter in MUPs

It is standard technique to use SF EMG data to evaluate NMJ function, but it is also possible to acquire individual MFPs using conventional CN electrodes. Attempts have been made to use conventional CN MUPs to measure and analyze neuromuscular jitter [25].

2.5.1 Using Filtered MUPs

For measuring neuromuscular jitter during voluntary contraction, at least two individual MFPs created by fibres in the same motor unit must be found. The larger the number of potentials, the easier it is to obtain potential pairs. Therefore, it would be advantageous to use a CN electrode to detect MUPs. CN electrodes, however, have a larger detection area than the SF electrode. The detected MUPs are therefore more often the superposition of individual MFPs, and the jitter seen may be a composite potential jitter. But some research has shown that apparent individual MFPs can be detected and estimates of the stability of MUPs can be obtained by using conventional CN electrodes and suitable filtering techniques.

Ertas [25] applied a CN electrode with a 2 kHz to 10 kHz bandpass filter to measure neuromuscular jitter in the extensor digitorum communis and orbicularis oculi muscles. He found that the potentials detected using a CN electrode resemble those detected using

a SF electrode with a 500 Hz to 10 kHz bandpass filter and that the results of the jitter measurement are highly comparable during voluntary contraction and electrical stimulation. However, when using a 500 Hz low-pass cut-off filter for CN electrodes, many of the detected potentials look wider than those detected using a SF electrode and superimposition occurs very frequently because of the larger detection area of the CN electrode compared to the SF electrode. Increasing the low-pass cut-off frequency from 500 Hz to 2 kHz can reduce the contributions of the low-frequency components of the action potentials of more distant muscle fibres. Although superposition of CN MUPs is more common than that of SF MUPs, the limitation of the superposition of individual MUPs can be eliminated to a great extent by discarding superimposed waveforms. Finally, Ertas concluded that the sensitivity of the CN electrode is almost equal to that of the SF electrode in detecting pathology. This means that using a CN electrode for neuromuscular jitter analysis may be an alternative to the SF electrode. CN electrodes give modestly higher numbers of potentials than SF electrodes and therefore require a lower contraction level. In addition, they are easier to operate, and much cheaper.

Buchman [26] measured neuromuscular jitter with standard SF EMG data techniques, except that a MN electrode was substituted for a SF electrode. He concluded that using MN EMG data for determining jitter studies is reproducible, can distinguish between normal subjects and those suffering from myasthenia gravis, and is more comfortable than using SF electrodes.

In fact, no matter what electrode type, only fibres in front of the detection surface contribute significant MFPs to MUPs. Although the number of fibres providing significant contributions to MUPs detected by a CN electrode is larger than those detected by a SF electrode, when only considering significant high frequency contributions, the difference in the number of fibres providing significant contributions is not very large because MFP amplitude, high frequency content and energy quickly decrease as the radial distance between the fibres and the electrode surface increases. Consequently, in high-passed-filtered CN MUPs, peaks for which the shape remains stable and which do not bifurcate across an ensemble of repeated discharges can be considered as individual muscle fibre contributions to the detected MUPs, and may be

therefore used for jitter measurements. However, for clinical use, data obtained using filtered CN MUPs must be compared with reference data based on CN MUPs and should not be compared with SF MUP based reference data. As with SF EMG data, to be confident that the individual MFP pairs are being considered, the peaks tracked throughout the ensemble of MUPs must be stable and not bifurcate.

2.5.2 Using MUP Acceleration

The accuracy of jitter measurements, whether based on CN or SF EMG data, depends on the extent to which significant individual fibre contributions can be correctly detected, i.e. the ability to detect individual MFPs in MUPs. Stashuk [28] proposed that using the MUP peak acceleration method detects significant individual MFP contributions to MUPs. Significant MFP contributions were represented by the detected peaks, with sufficient amplitude in the MUP accelerations, which were calculated using second-order difference equations. It was assumed that the detected peaks were created by contributions from individual fibres close to the detection surface of the electrode.

To quantitatively determine significant MFP contributions, simulation techniques were used and significant peaks in the MUP acceleration were defined using the MUP acceleration threshold. Based on the quantitative detection results, Stashuk concluded that analysing MUP acceleration is a powerful technique for detecting significant individual fibre contributions to MUPs and the significant peaks within the MUP accelerations can strongly correspond to individual fibre activity and may be useful for measuring neuromuscular jitter and fibre density [18].

2.6 Near MFP Contributions

Because the high frequency components and amplitudes of MFPs decrease quickly as the distance between the detection surface of the electrode and the muscle fibres increases, MFPs created by distant fibres have only very small contributions to the composite MUPs detected. The contributions are possibly smaller than those of the extraneous noise, and thus they will provide no useful information. Therefore, these MFPs provide no significant potential contributions to MUPs, and are usually referred to distant MFPs.

To measure neuromuscular jitter in MUPs, significant, i.e. near, MFP contributions have to be detected.

Ertas [25] considered only potentials with a stable shape, a rise time of less than 0.3 ms and an amplitude of more than 200 μV as near MFP contributions when he used filtered MUPs detected by CN electrodes to measure neuromuscular jitter.

Stashuk [18] defined detected peaks within the MUP acceleration, whose amplitude was greater than an expected threshold, as near MFP contributions when he used MUP acceleration to detect individual fibre contributions to MUPs.

In this thesis, near MFP contributions are defined as all expected MFP contributions that are created by fibres close to the detection surface of an electrode. Expected individual MFPs should have a relatively sharp waveform, relatively large amplitude and, short duration. They usually are composed of relatively high frequency components. Detected significant peaks that signify significant MFP contributions should have a stable shape with no bifurcation, a steep rise phase, and adequate amplitude across an ensemble of detected MUPs.

To measure neuromuscular jitter in MUPs, near MFP contributions have to be correctly identified. Depending on the frequency characteristics of near MFPs, suitable filtering techniques can be used to detect near MFP contributions. To prevent phase distortion, any filter used should have a linear or zero phase-shift in order to make the location of the detected peaks corresponding with that of the near MFP contributions. The filter should have good sensitivity for recognizing the character of the rapid rise time of near MFPs, and good selectivity for the designed frequency band. In addition, the chosen filter should be computationally efficient. The next chapter deals with detecting near MFP contributions using MUP acceleration in detail.

Chapter 3 Detecting Near Individual MFP Contributions to MUPs

3.1 Introduction

To measure neuromuscular jitter in MUPs, individual MFP contributions need to be detected in a quantitative way. The accuracy of a neuromuscular jitter measurement is dependent on the extent to which individual fibre contributions can be correctly detected. Detection of near MFP contributions should satisfy the following conditions:

a) Detected near MFP contributions should be created by corresponding near muscle fibres.

b) The maximal number of the near MFP contributions should be detected; and

c) As many as possible distant MFP contributions should be excluded.

In addition, detection results must be correctly evaluated. However, the exact MFP compositions of MUPs cannot be directly studied in actual muscles because biopsy data from specific MUs is not available. It is therefore impossible to exactly determine the MFP composition of real MUP data. Using simulated MUPs is a convenient, convincing and quantitative means of studying the features of composite MUPs and evaluating detection accuracy. It can help analyze the correlation between detected MFP contributions and the composition of the corresponding MUPs, and determine the reliability with which fibre contributions can be successfully detected. Therefore, MUPs with known MFP compositions have to be acquired in order to determine the accuracy of a detection technique. Consequently, it is necessary to develop simulated MUP data to help study the relationship between individual MFPs and composite MUPs.

As described in Chapter 1, MFP contributions to a MUP can be calculated based on the sizes and positions, relative to the detection electrode, of the muscle fibres of the MU. Based on the distribution of muscle fibres among the motor units of a muscle and their MFP contributions, MUPs can be calculated by adding MFPs for each MU. Then, according to each MU's firing times, MUPTs can be generated. Finally, simulated EMG signals are produced by superimposing the MUPTs of active MUs.

In this thesis, an EMG simulation system was used, which has been developed at the University of Waterloo by Dr. Dan Stashuk and his students. The system consists of four models: a muscle model, a MU recruitment and firing time model, a MFP and MUP model and a composite EMG signal model [27]. The muscle model defines the MU and muscle fibre distributions. The MU recruitment and firing time model determines which MUs of a muscle are active at a specific contraction level, and simulates firing times of the individual active MUs. In the MFP and MUP model, a line source volume conductor model is used to create MFPs and MUPs. MUPTs are produced using the firing times of the MUs. Finally, using the composite EMG signal model a simulated EMG signal is produced.

The simulated signals closely resemble real EMG signals at the most detailed level. The simulation system considers not only specific features of a muscle but also electrode configurations. Simulated EMG signals provide a basis for the quantitative assessment of MFP contributions to MUPs, and help improve the understanding of relationships between signal characteristics and detection parameters.

In real clinical settings, each MUP acquired using CN electrodes may consist of many (up to 50) individual MFP contributions [15]. However, a considerable portion of them are created by fibres that are relatively distant from the detection surface of the electrode, and would be defined as distant MFP contributions. To detect near MFP contributions, distant MFP contributions have to be minimized. As previously mentioned, distant MFP contributions relative to near MFP contributions usually consist of lower frequency components. Consequently, distant MFP contributions can be essentially removed by suitable filtering techniques, and thus near MFP contributions may be better detected.

To quantitatively determine the accuracy of detecting individual fibre contributions, MUPs of known MFP composition have to be available. By using simulated MUPs composed of specific known MFP contributions, the performance of filters can be analysed and compared, and the ability to identify near MFP contributions can be evaluated. According to specified evaluation criteria, filters can be developed, and

an optimal detection algorithm, which can most accurately detect near MFP contributions, can be determined.

3.2 Muscle Model

In order to simulate an EMG signal a model of the structure of a muscle is needed. The simulation algorithms accomplish this in several stages: muscle and motor unit territory diameter calculation; MU territory center location; fiber layout and assignment; and assignment of neuromuscular junction locations. They not only considers mathematical representations of overall statistical and spectral properties of detected EMG signals, but also individual MUP shapes, electrode and muscle configurations and MU firing times.

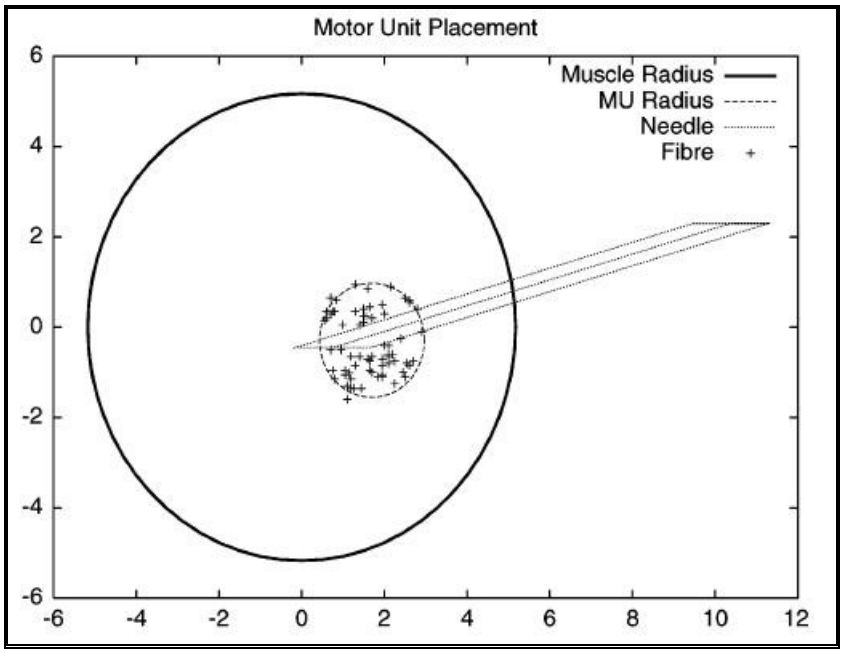

Figure 3.1 [34] Location of MU relative to needle electrode for one MU. Note that there is only one MU displayed here for simplification. Usually only fibres close to the centre of the needle tip will have significant contributions to a MUP, other fibres even close to cannula, are distant from the needle tip and their contribution to a MUP is usually small.

The muscle model can generate a population of muscle fibres of known size, position and motor unit membership, which is used to calculate the individual MFP contributions to composite MUPs and EMG signals. By using the muscle model, expected MFP contributions can be determined, and near and distant MFP contributions can be quantitatively defined.

3.3 Simulated MUPs

After the muscle model was defined, considering a specific detection electrode configuration, a simulated MUP was created for each of the active motor units. In this thesis, only SF and CN electrodes were considered. The detection surface of a CN electrode is elliptical with a major axis of 580 μm and a minor axis of 150 μm. Its major axis is aligned with the x-axis (the bottom of the detection area) and its minor axis was aligned parallel with the z-axis (the fibre direction). Only fibres in front of the detection surface were considered to contribute MFPs to MUPs. As presented in Chapter 2, however, the amplitudes of MFPs decrease quickly as the distances between the detection surface and the muscle fibres increase so that distant MFPs provide no significant potential contributions to MUPs. Therefore, it was useful to set up an arbitrary demarcation value to define an uptake area, and only fibres within the uptake area provided MFP contributions to MUPs. Therefore, MFPs that provided contributions to a MUP were created by fibres that belonged to the same MU, were in front of the detection surface and within the uptake area. Figure 3.2 illustrates an example for detecting expected MFP contributions to a MUP.

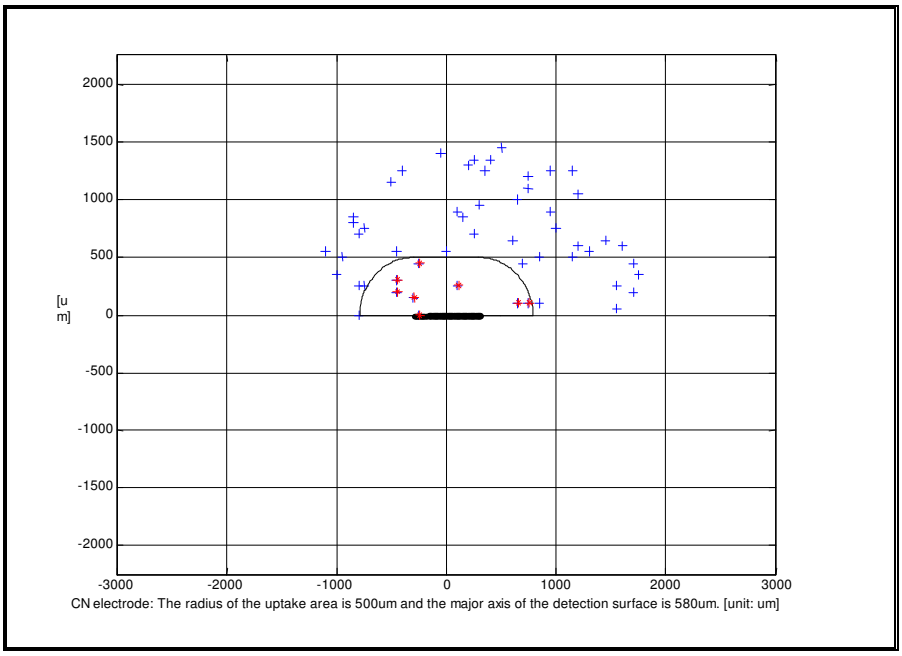

Figure 3.2 a: An active motor unit within the detection area. It contains 50 muscle fibres (marked by +), and 8 muscle fibres (marked by $*$) are within the uptake area of the electrode. These fibres are the expected fibres, and contribute MFPs to the composite MUP. The centre thick line represents the major axis of the electrode. The area enclosed by the thin line is the defined uptake area of the electrode.[8]

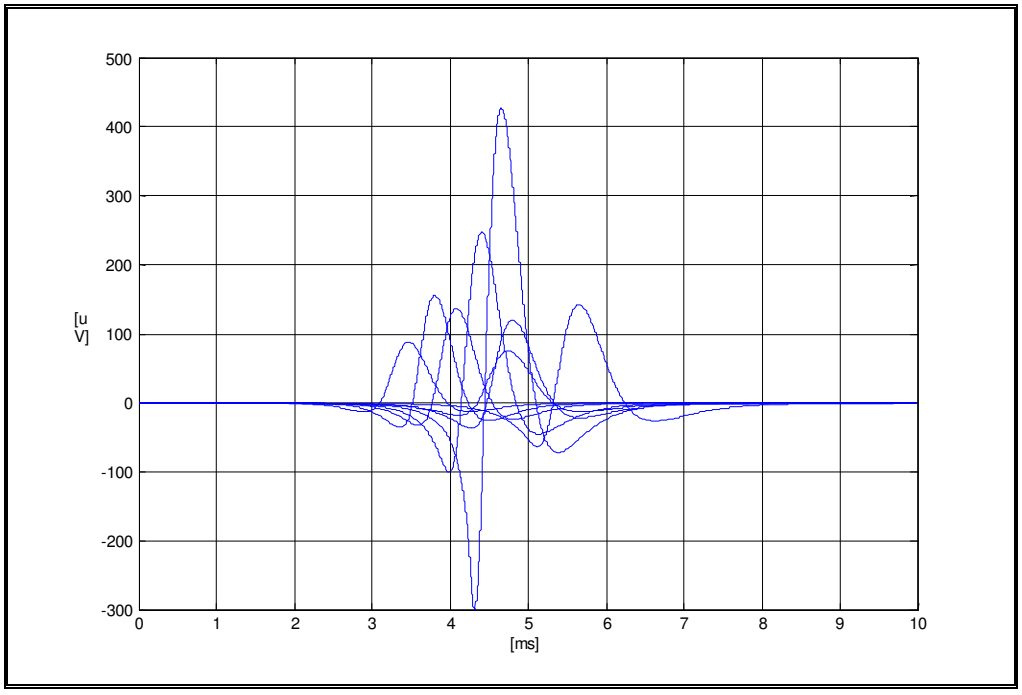

Figure 3.2 b: 8 MFPs generated by the 8 fibres described in Figure 3.2 a [8].

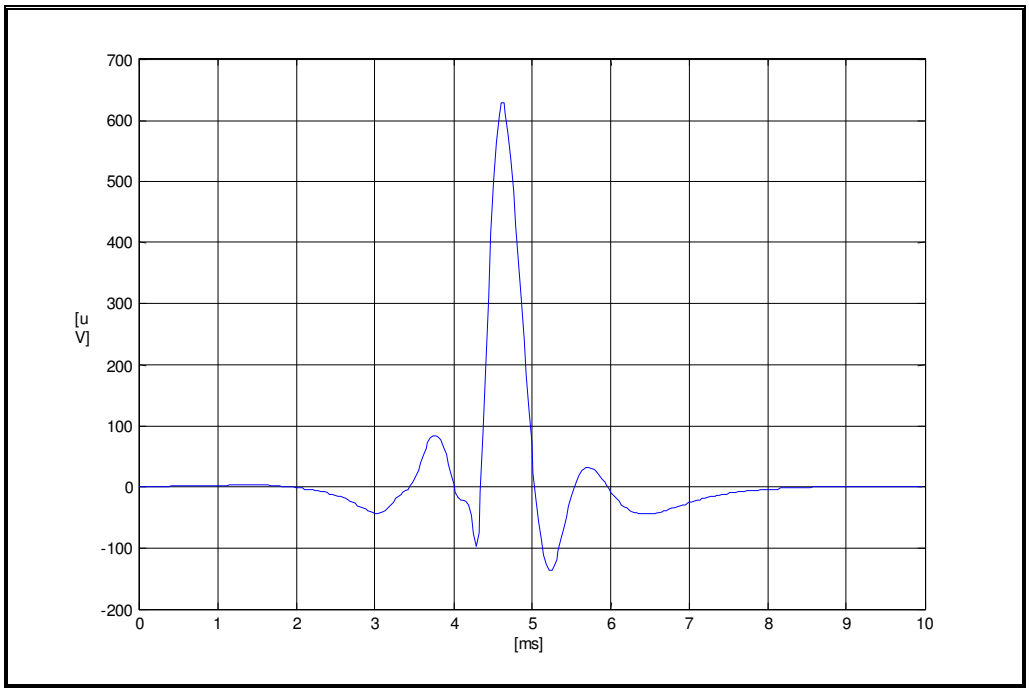

Figure 3.2 c: The composite MUP created by the summation of the MFPs described in Figure 3.2 b [8].

Each MFP was generated based on the line source volume conductor model. The line source model assumes that the muscle fibre is straight and cylindrical, and that the extra cellular medium is infinite with cylindrical anisotropy [9]. Based on the line source model, the action potential originates at the endplate and propagates along the axially directed fibres with a constant velocity, which is linearly related to the fibre diameter [14]. Figure 3.2 b demonstrates the expected MFP contributions from the active motor unit illustrated in Figure 3.2 a. In the simulation system, MFPs were simulated with a sampling rate of 937.5 kHz over an interval of 65.536 ms, so the simulated MFPs have a time resolution of about 1.067 μs.

A MUP is the summation of the expected MFPs contributed by fibres belonging to the same MU. Figure 3.2 c demonstrates a composite MUP from the MFP contributions shown in Figure 3.2 b.

3.4 MFP Library

In order to obtain MUPs composed of specific known MFPs, libraries of MFPs were established. Simulated EMG signals were created independently by the simulation

system for both CN and SF electrode. Except for the jitter value and the noise level, the same simulation parameters were used for creating the EMG signals. The important parameters were set as follows: 5.0% to 50% MVC contraction level, 100 motor units in muscle, max adoption distance 150 μm, needle position 15 mm from NMJ, signal to noise ratio 25, respectively.

The simulator was run several times and there were a total 50 active motor units in the simulated EMG signals. Therefore, 50 independent MUPs were created with more than 1000 distant and near, CN and SF MFPs. From these MFPs, 8 MFP libraries were established based on each different needle type and different acceleration thresholds. Namely Near25_CN, Near40_CN, Near25_SF, Near40_SF, Dist25_CN, Dist40_CN, Dist25_SF, Dist40_SF. In addition, 4 more, Dist5_CN, Dist10_CN, Dist5_SF and Dist10_SF, libraries were created to simulate distance fibre contributions. The number in the name means the acceleration threshold (kV/s^2) used to generate these libraries, it's the second derivative of the MFP signal and describes the sharpness of signal. For example Near25_CN represents a CN MFP library with maximum second derivative value larger than 25 kV/s^2, Dist25_SF means a SF MFP library with maximum second derivative value less than 25 kV/s^2. The assumption here is that near MFP contributions contain more high frequency signal components so they are sharper than distant ones. The amplitude of MFPs could also be used to define near and distant fibre firing, but since it ranges from several μV to up to 1000 μV for different size of common fibres, it was only used as a reference value. Compared to previous work [8], which used amplitude to define near and distance fibre contributions, the peak acceleration method gives more accurate results. This will be discussed in detail in chapter 4.

In the MFPs generated randomly by the simulation system, the maximum and minimum amplitudes of the Near25_CN MFPs are 291 μV, 93.6 μV respectively. The maximum and minimum amplitudes of the Near40_CN MFPs are 291 μV, 76.1 μV respectively. The MFP with the maximum amplitude should originate from the fibre located closest to the core of the detection electrode, and can be considered an MFP on the 100% isopotential, and the MFP with the minimum amplitude is generated by athe

fibre very close to the edge of the design uptake radius (500 μm). Complete Max and Min values for different fibre libraries are listed below (Table 3.1).

CN	near 40	near 25	dist 40	dist 25
max (mv)	0.291	0.291	0.109	0.0808
min (mv)	0.0936	0.0761	0.038	0.038
SF	near 40	near 25	dist 40	dist 25
max (mv)	0.4025	0.4025	0.1377	0.1121
min (mv)	0.0769	0.0645	0.0395	0.0395

Table 3.1: Max and Min values of CN and SF MFP libraries.

Based on the 25 and 40 kV/s^2 threshold for the peak acceleration of near MFPs, the MFP library was divided into 2 sub-libraries: the near MFP library with derivative value above threshold and the distant MFP library with values below threshold. The near MFPs can provide contributions that should be able to be consistently detected in a composite MUP. The distant MFPs provide contributions to MUPs, which are not expected to be able to be consistently detected and resemble interference or noise. There are 102 MFPs in the near40 MFP library and 173 MFPs in the near25 MFP library. Because of the large number of distant MFPs, 200 MFPs were randomly chosen to put into each library. Using the concepts of near and distant MFP contributions the MFP contributions which can be expected to be detected in MUPs can be determined. Using the MFP libraries, specific MUP sets were generated to do further study, details are discussed in Chapter 4.

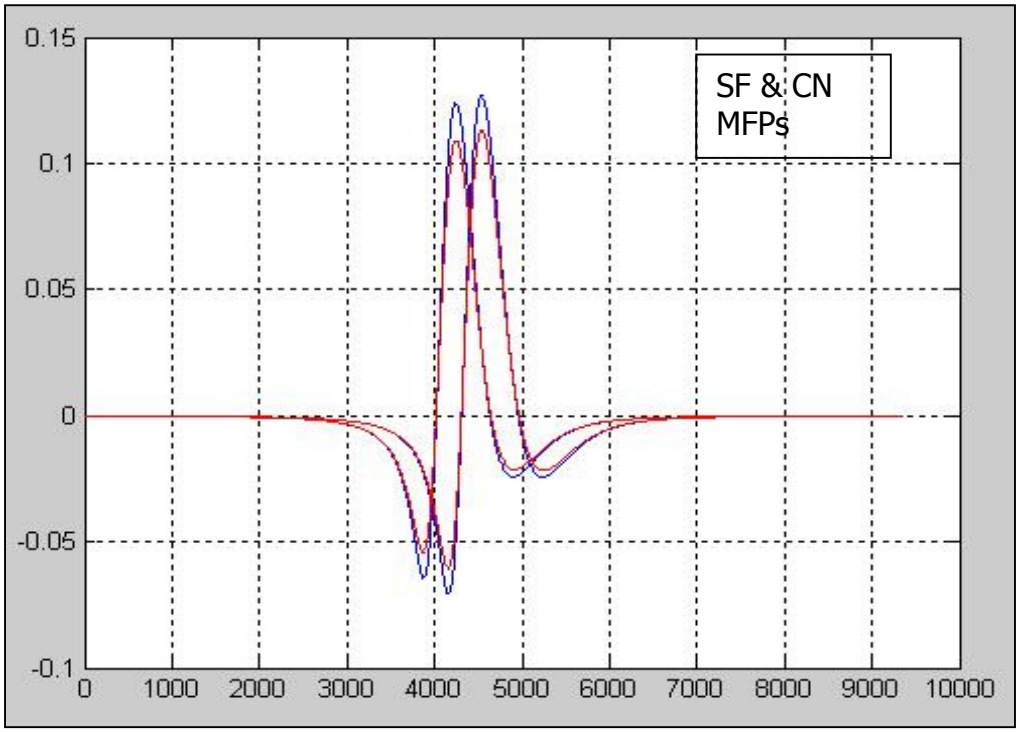

Figure 3.3: Sample wave forms from MFP libraries; the two larger ones are SF MFPs and the two smaller ones are CN MFPs. Generally SF MFPs are larger and sharper than CN MFPs so they are more easily detected.

3.5 Frequency Spectrum Analysis of Individual MFPs and MUPs

Features of the frequency spectrum of EMG signals have been researched for a long time. But most researchers focus on investigating the correlation between neuromuscular features and the frequency spectrum of corresponding EMG signals. It has been established that the frequency spectrum of a normal EMG signal acquired using needle electrodes usually has a range of main power components from 10 to 2000 Hz, and its largest peak is around 100 Hz [28]. This result indicates that an EMG signal contains more low frequency content than high frequency content. These results can be used for near MFP detection. To detect near MFP contributions, the frequency spectra of the individual MFPs has to be analyzed.

As presented in section 3.4, the objective is to distinguish between near and distant MFP contributions with sharpness thresholds of 25 or 45 kV/s^2 respectively. Visually analyzing frequency spectra estimates of simulated MFPs with various amplitudes, it was found that their frequency spectra have very similar shapes at low frequencies and that their primary difference is at high frequencies (see Figure 3.4). The peak of their spectrum estimates was between 500 Hz and 1100 Hz. Moreover, the greater the amplitude of a MFP, the larger its spectral density, the higher the frequency of the position of its spectral peak and the slower the declination of its spectral density as frequency increases.

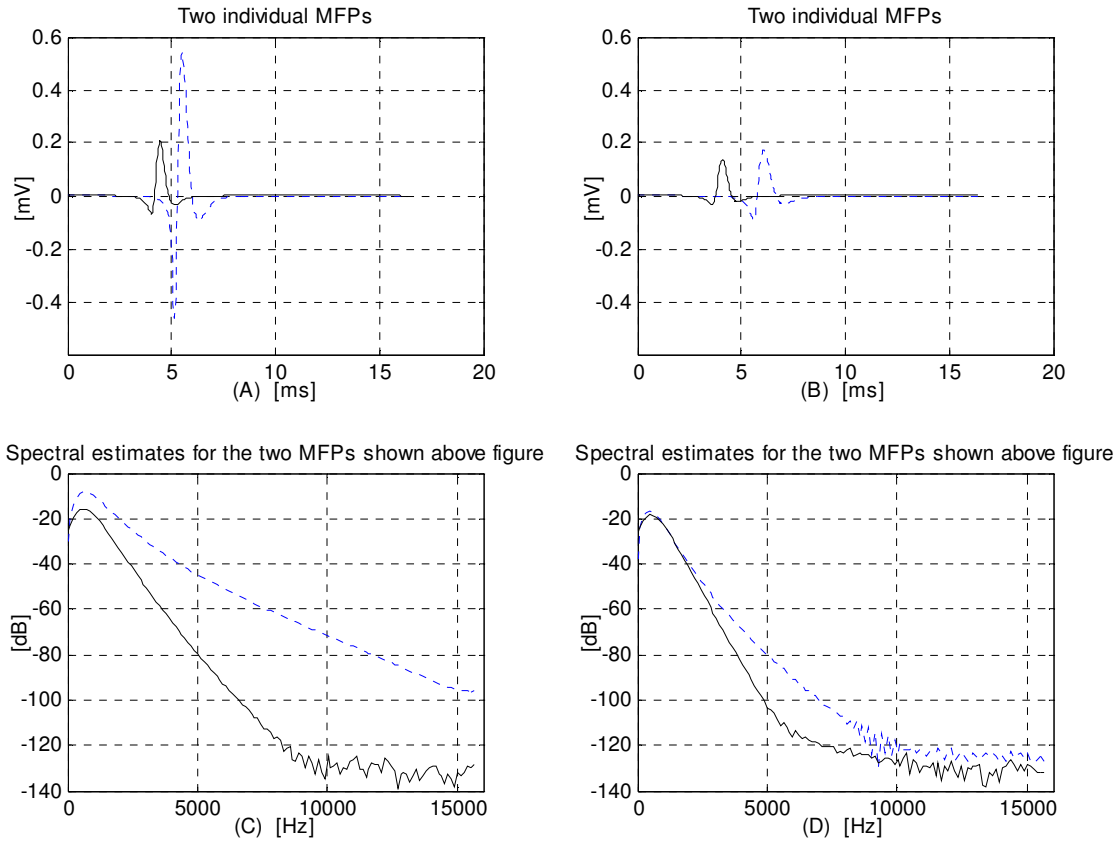

Figure 3.4 Individual MFPs and their spectral estimates[8]

(A): The amplitude of the MFPs represented by the dotted and solid line is 500 μV and 200 μV, respectively. (C) is their corresponding spectral estimates. (B): The amplitude of the MFPs represented by the dotted and solid line is 170 μV and 140 μV, respectively. (D) is their corresponding spectral estimates.

From previous work on analyzing frequency spectra of real and simulated individual MUPs, it was found that the features of their spectral estimates were similar to those of the individual MFPs. The bandwidth below 2000 Hz always contained the dominant spectral energy with the largest peak. Between 2000 Hz and 3500 Hz, the spectral density was relatively low. Over 3500 Hz, the spectral density and its changes were small.

Therefore, for an individual MUP, the large peak of the spectral density means that there are lots of MFP contributions in the low frequency bandwidth (below 2000 Hz).

These contributions may contain mostly distant MFP contributions with relatively low frequency components. In the high frequency zone (3500 Hz to 10 kHz), there is a low and approximately constant spectral density, so individual MFP contributions to the MUPs in this frequency range are few and most of the energy comes from noise (the spectral density of individual MFPs is relatively low and rapidly falls off over 3500 Hz). Therefore, the meaningful frequency section, which can be used to detect near MFP contributions, should be between 2000 Hz and 3500 Hz. This relatively high frequency range contains energy, which mainly comes from near MFP contributions, because most of the energy of distant MFP contributions is not in this bandwidth. Therefore, using suitable bandpass filters can reduce unwanted spectral components such that near MFP contributions can be detected. Reasonable high and low pass cut-off frequencies of such filters should be 2000 Hz and 3500 Hz respectively.

3.6 Choice of the Filters

Based on previous work and current industry practice, several filters were chosen for near MFP detection. To correctly detect individual MFP contributions, the filters used required a linear phase response to assure that the detected contributions accurately represented the temporal locations of the corresponding MFP contributions. The ability of a filter to detect near MFP contributions in MUPs was evaluated using the following criteria:

a) The sharpness and amplitude of detected significant peaks (which represent near MFP contributions).

b) Supression of false peaks generated by the filter, distant MFP contributions and noise.

c) Adaptability and temporal resolution of filter (in order to accommodate biological variations of MUPs).

d) Time required to complete MFP detection (must be clinically reasonable 1 – 5 s).

3.6.1 Zero-phase Butterworth Filters

The Butterworth filter is a typical classical IIR filter. Its magnitude response is smooth over the complete bandwidth. Based on the passband width requirements, zero-phase bandpass Butterworth filters were designed by using MATLAB software, and used to detect near MFP contributions in MUPs.

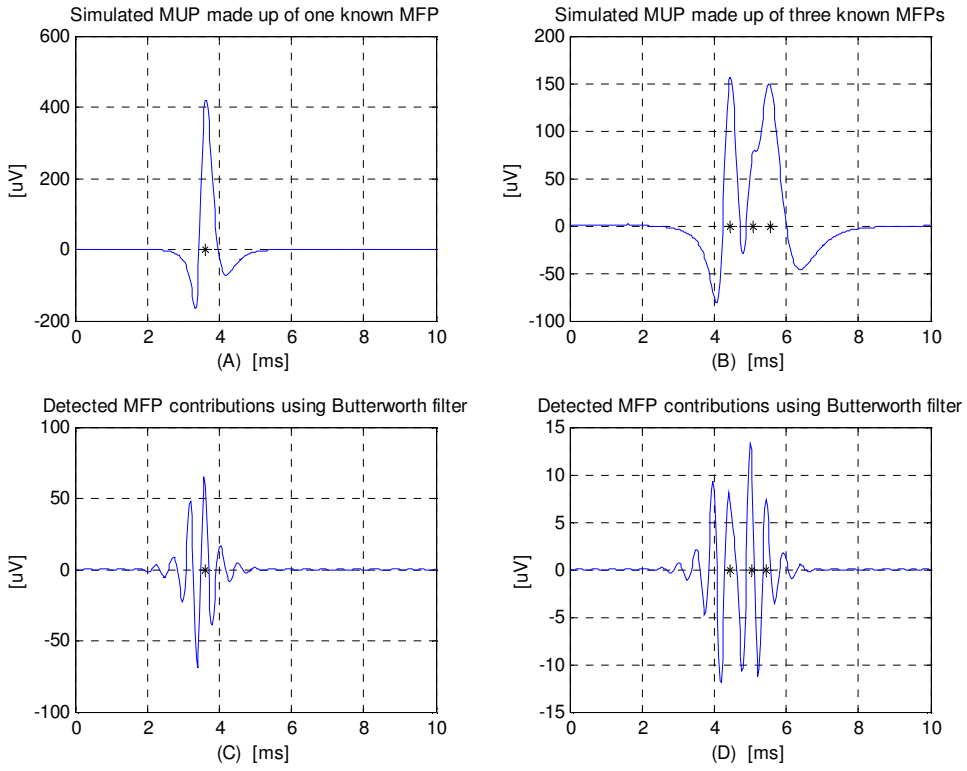

Figure 3.5: Using a 2-order zero-phase Buttereworth bandpass filter (2000Hz to 3500Hz) MFP contributions in MUPs are detected. (Mark '*' represents the peak locations of near MFP contributions. In (C) and (D), the first big peaks are false peaks.) [8]

Through a series of simulation experiments, it was found that it is difficult to use the bandpass Butterworth filter with a suitable bandwidth and order to identify near MFP contributions in MUPs. In general, there were too many false peaks in the filtered MUPs. A wider bandwith can be used to reduce the ringing effect, but the time resolution suffers.

Figure 3.5 provides two examples for detecting MFP contributions in simulated MUPs by using a 2nd-order zero-phase bandpass Butterworth filter.

3.6.2 The McGill Filter

Stashuk [18] used MUP acceleration to detect near MFP contributions to MUPs. He defined a near MFP contribution as one with the peak MUP acceleration above an expected threshold. MUP accelerations were achieved by calculating a second-order difference equation. The difference equation was derived from a difference filter used by McGill [32], so it is named the McGill filter in this thesis. The McGill filter is a second-order differentiator, a symmetric FIR filter. Its equation is as follows:

$$Y_n = \frac{1}{3}X_{n+6} - \frac{1}{3}X_{n+3} - \frac{1}{3}X_n + \frac{1}{3}X_{n-3}$$

where: X_n is the sampled data of the original signals;
Y_n is the data of the filtered MUP.

The McGill filter is convenient to implement, and has good temporal resolution resulting from the short sampling data length used. From the time-domain point of view, it computes approximations of the second-order derivative of the input signal. It can therefore accentuate the rapid rising edges of the MUPs, and convert them into narrow spikes. Since near MFPs usually have a sharp peak, use of the McGill filter may be efficient for detecting their contributions in MUPs. From the frequency-domain point of view, the McGill filter is a bandpass filter. It suppresses high-frequency noise and low-frequency background activity, such as distant MFP contributions and noise. Figure 3.9 is the magnitude response of the McGill filter. As can be seen, the McGill filter is a multiband bandpass filter for a 31.25 kHz sampling rate. For the first passband, the cut-off frequencies are 2000 Hz and 4250 Hz, and the centre frequency is 3150 Hz. However, the other two high frequency passbands are not desired as they make the filter more sensitive for high frequency noise.

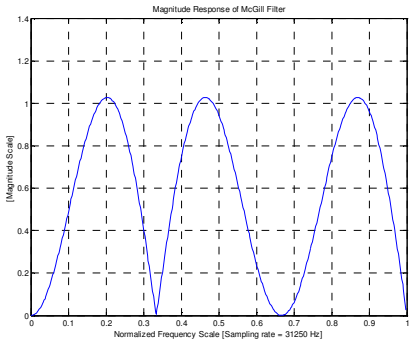

Figure 3.6 a: The magnitude response of the McGill filter. The first passband is from 2000 Hz to 4250 Hz, and the centre frequency is 3150 Hz.[8]

3.6.3 Acceleration filter

One previous work [8] proposed another filter derived from the McGill filter. Based on the least-squares criteria and a passband requirement of 2000 Hz – 3500 Hz, a 2nd-order differentiator was designed as follows:

$$\begin{aligned} Y_n = &- 0.2158*X_n - 0.15207*(X_{n+1} + X_{n-1}) - 0.04439*(X_{n+2} + X_{n-2}) \\ &+ 0.042743*(X_{n+3} + X_{n-3}) + 0.088353*(X_{n+4} + X_{n-4}) + 0.10395*(X_{n+5} + X_{n-5}) \\ &+ 0.075737*(X_{n+6} + X_{n-6}) + 0.017537*(X_{n+7} + X_{n-7}) - 0.015467*(X_{n+8} + X_{n-8}) \\ &- 0.012167*(X_{n+9} + X_{n-9}) + 0.003664*(X_{n+10} + X_{n-10}) \end{aligned}$$

This 2nd-order differentiator is named the Acceleration filter. Figure 3.11 shows its magnitude response. Its cut-off frequencies are 2000 Hz and 4100 Hz, and the centre frequency is 3050 Hz. The passband requirement of 2000 Hz – 3500 Hz can be approximately satisfied and it has a minimum data length for the corresponding filter order. Compared with the 1st-order differentiator, it has a similar frequency response, but the data length of the 2nd-order differentiator is longer. The Acceleration filter also has a shift between the locations of the detected peaks and the locations of the corresponding contributing MFP peaks (See Figure 3.6b).

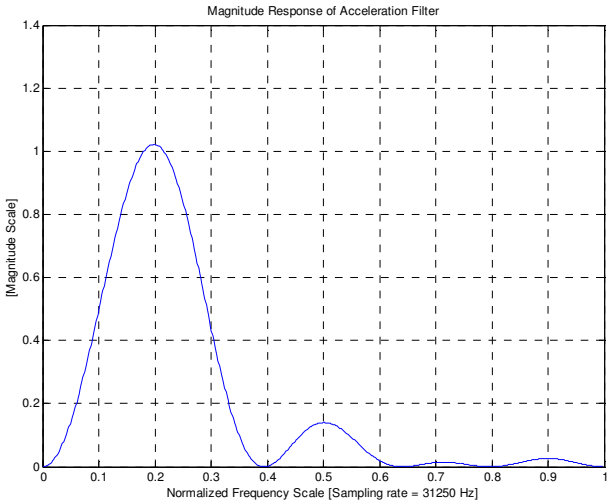

Figure 3.6b The magnitude response of the Acceleration filter. The passband is from 2000 Hz to 4100 Hz, and the centre frequency is 3050 Hz. [8]

3.7 Identifying Features of Near MFP Contributions

To clearly identify near MFP contributions in MUPs, a filter must have a good ability to accurately differentiate between significant and false peaks. In some sense, this is difficult because the definition of near MFP contribution is in itself somewhat arbitrary. In previous work [8] an amplitude threshold was defined to distinguish near and distant MFP contributions. In section 3.4, for instance, near MFP contributions were defined as all the expected MFPs that have 25 and 40 kV/s^2. According to this definition, we set up a near MFP and distant MFP library. However, the individual MFPs may contain different frequency content, and the sharpness of their peaks may be different. To detect near MFP contributions as accurately as possible, reasonable detection parameters and thresholds have to be defined. The proposed method is to use CN EMG to get as good as, or close to, jitter estimate performance as does traditional SF EMG, so an analysis on both CN and SF MFP libraries was performed.

Based on the analysis of the peak features of the filtered MUPs, three detection parameters: amplitude, sharpness and slope ratio, were used. In addition, the locations of the detected peaks were also used to help confirm the correctness of the detection results. Here, the amplitude refers to the magnitude of the detected peaks. The sharpness relates

to how sharp the peak is, and is defined as the minimum of the slope of the rising and falling edges. The slope ratio is the ratio of the falling slope to rising slope, it describes the symmetry of the filtered spike. The slope was defined as the amplitude variation per unit time. However, n fact, the amplitude variation per unit time is actually not often consistent. To measure the sharpness feature as accurately as possible, the slope was calculated by an algorithm, generally if the rise and fall amplitudes of a spike are close to the same value then the slope is calculated using all of the spike data, if not only data close to the peak of the spike is used to calculate the slope ratio.

After the three detection parameters were defined, all individual MFPs from the near and distant MFP libraries were used to claculate these parameters in order to identify the features of near MFP contributions. In addition, the shift of the detected peaks and the ratio of the amplitude of the maximum false peak to the amplitude of the smallest true peak, called the false-to-true peak ratio, were also analysed. Table 3.2 shows the results from the analysis of two near and distant MFPs libraries using the McGill filter.

McGill filter and 25CN_lib		Peaks representing near MFP contributions from the near MFP library	Peaks representing distant MFP contributions from the distant MFP library	False peaks created from near MFP contributions from the near MFP library
Amplitude [μV]	Mean	102.7	23.5	19.3
	Max	321.8	42.2	57.6
	Min	43.6	11.8	9.21
Sharpness [μV/μs]	Mean	0.731	0.125	0.051
	Max	2.771	0.257	0.18
	Min	0.263	0.051	0.02
Slope ratio	Mean	1.416	1.59	0.35
	Max	1.672	2.03	0.42
	Min	1.085	1.24	0.30
Shift [Sampling unit]	Mean	-12.1	-12	
	Max	-10	-12	
	Min	-13	-15	
False-to-true peak ratio (%)	Mean			21.3
	Max			29.9
	Min			11.9

Table 3.2a: The results from analyzing all 173 near and 185 distant MFP contributions using the McGill filter on the 25CN_LIB MFP library.

McGill filter and 40CN_lib		Peaks representing near MFP contributions from the near MFP library	Peaks representing distant MFP contributions from the distant MFP library	False peaks created from near MFP contributions from the near MFP library
Amplitude [μV]	Mean	143.3	28.2	25.2
	Max	307.2	67.2	57.6
	Min	67.3	11.8	13.1
Sharpness [μV/μs]	Mean	1.094	0.157	0.068
	Max	2.771	0.446	0.18
	Min	0.384	0.051	0.03
Slope ratio	Mean	1.371	1.57	0.35
	Max	1.595	2.03	0.42
	Min	1.085	1.24	0.30
Shift [Sampling unit]	Mean	-11.6	-13.4	
	Max	-10	-11	
	Min	-13	-15	
False-to-true peak ratio (%)	Mean			18.7
	Max			24.5
	Min			11.9

Table 3.2b: The results from analyzing all 103 near and 185 distant MFP contributions using the McGill filter on the 40CN_LI B MFP library.

To have a better understanding of the Table 3.2 data, we plot them in the following figures, "*" represents near MFP data; "+" represents distant MFP data and "o" represents false peak data generated by the filter.

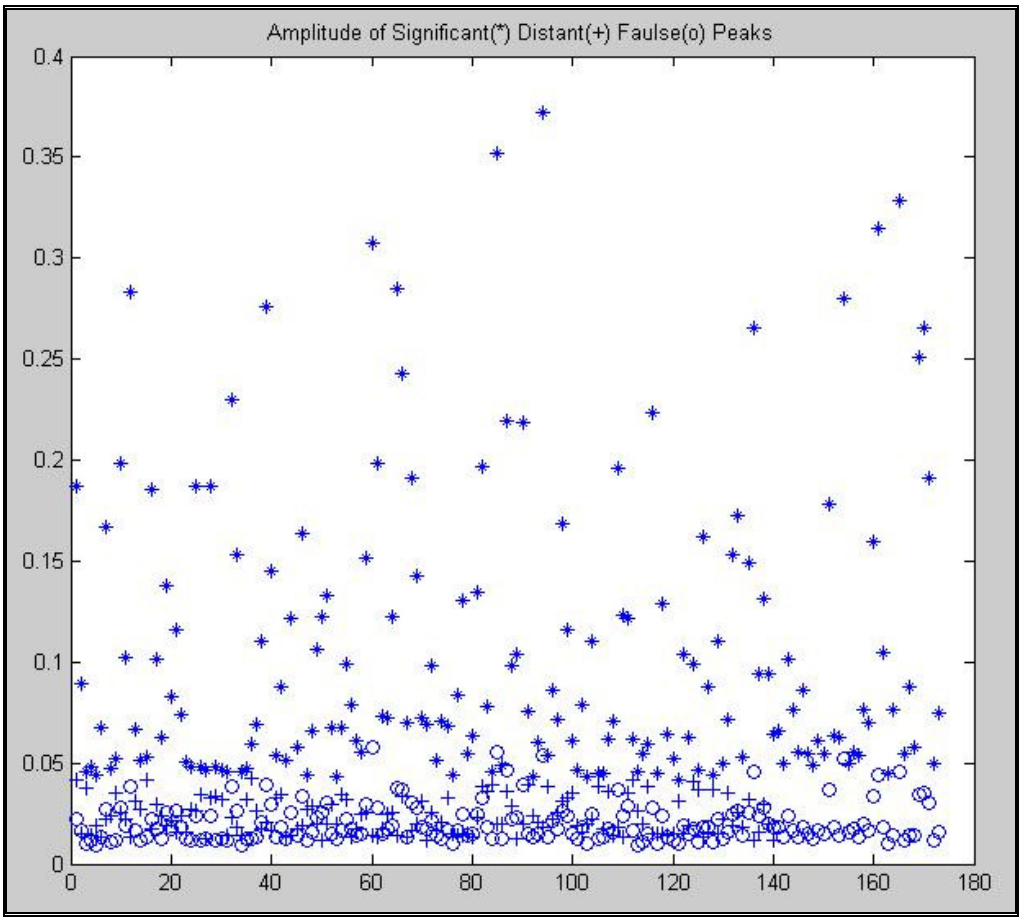

Figure 3.7a Amplitudes of peaks in Table 3.2, though we can see most near (significant) peaks are much bigger than false and distant peaks, some of them are overlapped. So it is difficult to use amplitude only to distinguish true and false peaks.

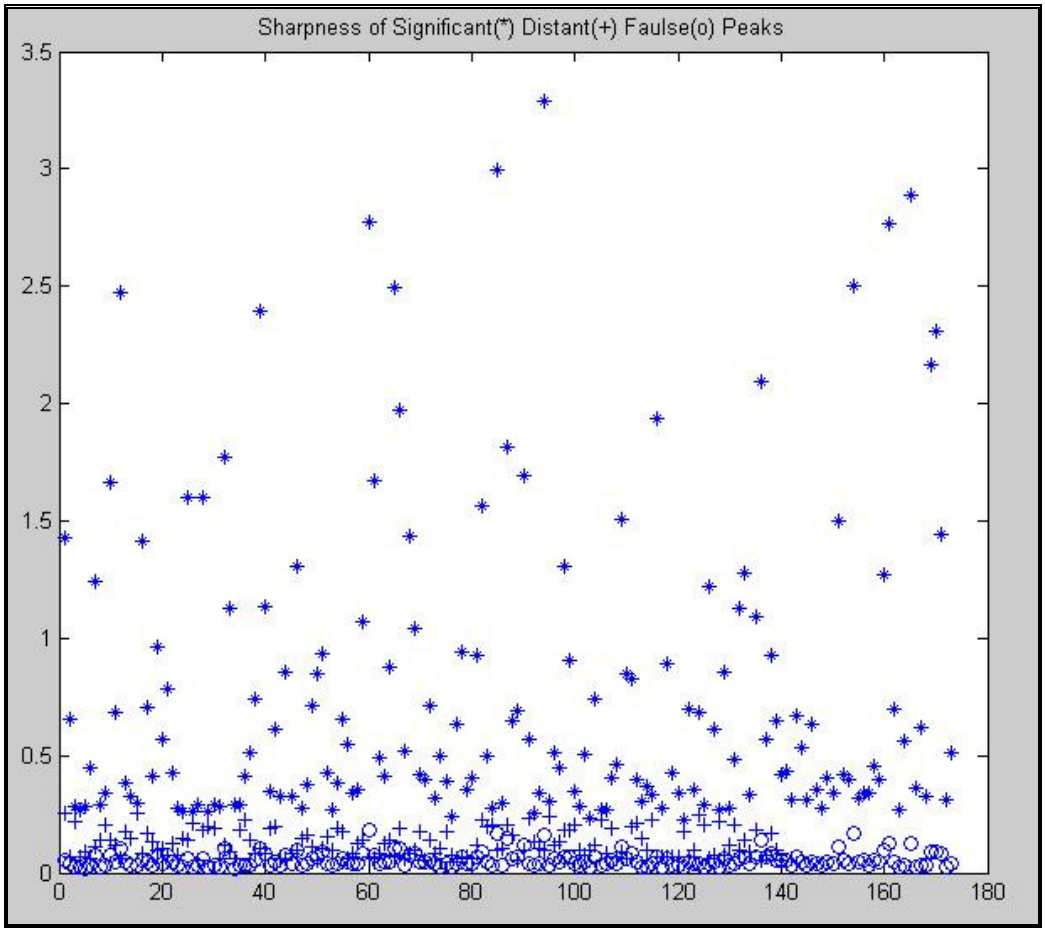

Figure 3.7b Sharpness of peaks in Table 3.2, we can separate near and false peaks easily using a sharpness threshold, and maybe also near and distant peaks.

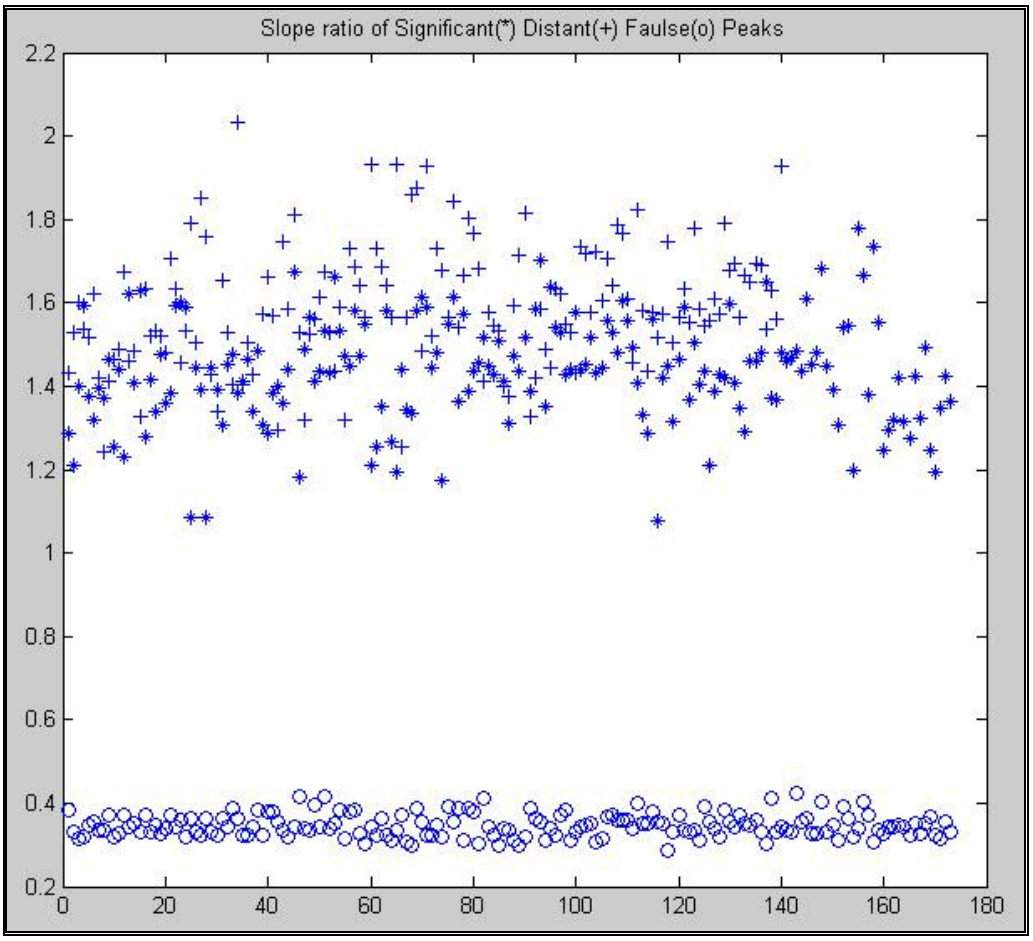

Figure 3.7c Slope ratio of peaks in Table 3.2, though near and distant MFP data are mixed together, we can easily separate false peaks by using a slope ratio threshold.

Examining Table 3.2 and Figure 3.7, we found that near and distant MFP contributions can be differentiated using slope ratio and sharpness. Compared with the distant and false MFP contributions, the near ones usually have large sharpness and better symmetry, which is measured by the slope ratio. The chosen thresholds should be able to exclude almost all distant MFP contributions, and only remove a few near MFP contributions. Since we want no false peaks and can tolerate some distant MFPs, we chose the mean value as the detection threshold. Amplitude was only used as a reference value because its value overlapped with false and true peaks. Although the McGill filter has a mean false-to-true peak ratio of 24.5%, the amplitude of a large false peak may be larger than that of a small true peak. Fortunately, the problem of false peaks can be solved using the slope ratio. All near peaks have a relatively high slope ratio, which

means that peaks of near and distant MFP contributions usually have steeper falling edges than their rising edges. However, the case for false peaks is just the reverse. The positions of the positive peaks of the filtered MUPs are used to represent the temporal locations of the MFP contributions. However, the temporal locations of the positive peaks correspond with the starting points of the rising edges of MFP contributions, not with their peaks. In addition, distant MFP contributions often have a greater shift than near MFP contributions. Therefore, a shift was considered when we analysed the accuracy of the detection results.

Accel filter and 25CN_lib		Peaks representing near MFP contributions from the near MFP library	Peaks representing distant MFP contributions from the distant MFP library	False peaks created from near MFP contributions from the near MFP library
Amplitude [μV]	Mean	102.7	23.8	19.6
	Max	321.8	43.5	58.5
	Min	43.6	11.9	9.29
Sharpness [μV/μs]	Mean	0.744	0.127	0.052
	Max	2.764	0.267	0.188
	Min	0.235	0.052	0.021
Slope ratio	Mean	1.395	1.58	0.34
	Max	1.704	1.95	0.44
	Min	1.119	1.16	0.28
Shift [Sampling unit]	Mean	-10.5	-12	
	Max	-12	-14	
	Min	-8	-10	
False-to-true peak ratio (%)	Mean			21.1
	Max			29.8
	Min			11.8

Table 3.3 a: The results from analyzing all near and distant MFP contributions using the Acceleration filter on the 25CN_LIB MFP library.

Accel filter and 40CN_lib		Peaks representing near MFP contributions from the near MFP library	Peaks representing distant MFP contributions from the distant MFP library	False peaks created from near MFP contributions from the near MFP library
Amplitude [μV]	Mean	146.3	28.8	25.6
	Max	321.8	67.6	58.5
	Min	69.3	11.9	13.3
Sharpness [μV/μs]	Mean	1.1	0.162	0.069
	Max	2.76	0.444	0.188
	Min	0.46	0.052	0.032
Slope ratio	Mean	1.36	1.56	0.34
	Max	1.7	1.95	0.44
	Min	1.12	1.16	0.28
Shift [Sampling unit]	Mean	-10	-11.9	
	Max	-8	-10	
	Min	-12	-14	
False-to-true peak ratio (%)	Mean			15.6
	Max			24.3
	Min			11.8

Table 3.3 b: The results from analysing all near and distant MFP contributions using the Acceleration filter on the 40CN_LIB MFP library.

Table 3.3 show results from analyzing the individual MFPs using the Acceleration filter. Similar to the McGill filter results, the detection thresholds for the Acceleration and Slope filters can be determined based on Table 3.3 a and b. Referring to Table 3.2 and 3.3, there are very similar features between the detection results of the McGill and Acceleration filters. For the Acceleration filter, the thresholds of its detection parameters are basically the same as those of the McGill filter, and the thresholds of the sharpness and slope ratio can also be chosen around the mean distant MFP values.

Below are data generated from different bandwidth Butterworth filters, we tried the same bandwidth as that of the McGill filter and other currently widely used bandwidths.

ButterWorth filter and 25CN_lib 2k~3.5k		Peaks representing near MFP contributions from the near MFP library	Peaks representing distant MFP contributions from the distant MFP library	False peaks created from near MFP contributions from the near MFP library
Amplitude [μV]	Mean	12.1	1.48	10.8
	Max	48.4	4.99	42.2
	Min	3.8	0	3.45
Sharpness [μV/μs]	Mean	0.123	0.141	0.113
	Max	0.492	0.2053	0.453
	Min	0.037	0.0	0.036
Slope ratio	Mean	0.785	0.487	0.34
	Max	1.336	0.94	0.44
	Min	0.643	0	0.28
Shift [Sampling unit]	Mean	-4.2	-2.2	
	Max	-2	-0	
	Min	-17	-6	
False-to-true peak ratio (%)	Mean			1.3
	Max			1.69
	Min			0.61

Table 3.4 a: The results from analysing all near and distant MFP contributions using the 2khz to 3.5khz band pass Butterworth filter on the 25CN_LIB MFP library. We can see false peaks created by the filter have almost the same amplitude, sharpness and slope ratio values as peaks created by real MFPs, so we can not use this bandwidth to detect near fibre contributions.

ButterWorth filter and 40CN_lib 2k~3.5k		Peaks representing near MFP contributions from the near MFP library	Peaks representing distant MFP contributions from the distant MFP library	False peaks created from near MFP contributions from the near MFP library
Amplitude [μV]	Mean	18.2	2.08	16.4
	Max	48.4	7.86	42.2
	Min	6.96	0	6.07
Sharpness [μV/μs]	Mean	0.188	0.02	0.172
	Max	0.492	0.07	0.453
	Min	0.065	0.0	0.061
Slope ratio	Mean	0.809	0.533	1.26
	Max	1.336	0.94	1.63
	Min	0.643	0	0.61
Shift [Sampling unit]	Mean	-4.7	-2.4	
	Max	-2	-0	
	Min	-17	-6	
False-to-true peak ratio (%)	Mean			0.89
	Max			0.96
	Min			0.83

Table 3.4 b: The results from analyzing all near and distant MFP contributions using the 2khz to 3.5khz band pass Butterworth filter on the 40CN_LIB MFP library, are the same as above, false peaks created by the filter have almost the same amplitude, sharpness and slope ratio values as peaks created by real MFPs, so we can not use this bandwidth to detect near fibre contributions.

Butterworth filter and 25CN_lib 2k~10k		Peaks representing near MFP contributions from the near MFP library	Peaks representing distant MFP contributions from the distant MFP library	False peaks created from near MFP contributions from the near MFP library
Amplitude [μV]	Mean	13.3	2.66	8.2
	Max	50.4	6.69	28.5
	Min	4.7	0	2.66
Sharpness [μV/μs]	Mean	0.091	0.018	0.055
	Max	0.367	0.046	0.198
	Min	0.031	0.0	0.016
Slope ratio	Mean	0.589	0.608	2.49
	Max	0.708	0.848	3.22
	Min	0.468	0	1.39
Shift [Sampling unit]	Mean	-2.8	-2.5	
	Max	-2	-0	
	Min	-4	-5	
False-to-true peak ratio (%)	Mean			0.58
	Max			0.93
	Min			0.4

Table 3.4 c: The results from analyzing all near and distant MFP contributions using the 2khz to 10khz band pass Butterworth filter on the 25CN_LIB MFP library. The sharpness and slope ratio values can be used to separate false peaks from those created by near MFP contributions.

ButterWorth filter and 40CN_lib 2k~10k		Peaks representing near MFP contributions from the near MFP library	Peaks representing distant MFP contributions from the distant MFP library	False peaks created from near MFP contributions from the near MFP library
Amplitude [μV]	Mean	19.2	2.08	12.4
	Max	50.4	7.86	28.5
	Min	8.42	0	4.61
Sharpness [μV/μs]	Mean	0.133	0.02	0.085
	Max	0.367	0.07	0.198
	Min	0.055	0.0	0.029
Slope ratio	Mean	0.557	0.533	2.54
	Max	0.68	0.94	3.22
	Min	0.468	0	1.39
Shift [Sampling unit]	Mean	-2.8	-2.4	
	Max	-2	-0	
	Min	-4	-6	
False-to-true peak ratio (%)	Mean			0.63
	Max			0.93
	Min			0.50

Table 3.4 d: The results from analyzing all near and distant MFP contributions using the 2khz to 10khz band pass Butterworth filter on the 40CN_LIB MFP library.

Butterworth filter and 25CN_lib 500~10k		Peaks representing near MFP contributions from the near MFP library	Peaks representing distant MFP contributions from the distant MFP library	False peaks detected with near MFP contributions from the near MFP library
Amplitude [μV]	Mean	94	36.5	7.0
	Max	221.5	55.5	13.6
	Min	53.3	23.1	3.6
Sharpness [μV/μs]	Mean	0.365	0.135	0.01
	Max	0.985	0.237	0.02
	Min	0.185	0.077	0.005
Slope ratio	Mean	0.564	0.583	2.78
	Max	0.7	0.689	3.10
	Min	0.473	0.496	2.52
Shift [Sampling unit]	Mean	-0.18	-0.25	
	Max	-0	-0	
	Min	-1	-1	
False-to-true peak ratio (%)	Mean			0.07
	Max			0.1
	Min			0.05

Table 3.4 e: The results from analyzing all near and distant MFP contributions using the 500hz to 10khz band pass Butterworth filter on the 25CN_LIB MFP library.

Butterworth filter and 40CN_lib 500~10k		Peaks representing near MFP contributions from the near MFP library	Peaks representing distant MFP contributions from the distant MFP library	False peaks detected with near MFP contributions from the near MFP library
Amplitude [μV]	Mean	121	40.9	8.7
	Max	221.4	77.1	13.6
	Min	69.5	23.1	5.47
Sharpness [μV/μs]	Mean	0.475	0.153	0.0129
	Max	0.985	0.307	0.02
	Min	0.26	0.077	0.008
Slope ratio	Mean	0.551	0.583	2.84
	Max	0.631	0.7	3.10
	Min	0.473	0.496	2.60
Shift [Sampling unit]	Mean	-0.19	-0.24	
	Max	-0	-0	
	Min	-1	-1	
False-to-true peak ratio (%)	Mean			0.07
	Max			0.1
	Min			0.05

Table 3.4f: The results from analyzing all near and distant MFP contributions using the 500hz to 10khz cut band ButterWorth filter on 40CN_LIB MFP library.

We applied different band pass Butterworth filters to Near and Distant MFP libraries in Table 3.4. The reason is that the Butterworth filter is currently widely used for SF EMG signal analysis. So we needed to compare the result with our method to show if it gets better results. Like the McGill and Acceleration filters, using differences in amplitude, sharpness and symmetry near and distant MFP contributions can be identified. For the Butterworth filer, we need to use a 500 to 10k or 2k to 10k band pass to reduce the ringing effect, so we can apply this filter in MFP detection.

In order to compare SF filtered data, we also applied different filters to SF libraries. Table 3.5 shows the data.

McGill filter and 25 SF_lib		Peaks representing near MFP contributions from the near MFP library	Peaks representing distant MFP contributions from the distant MFP library	False peaks created from near MFP contributions from the near MFP library
Amplitude [μV]	Mean	116.7	24.9	22.5
	Max	591.3	69.7	79
	Min	27.1	11.5	7.6
Sharpness [μV/μs]	Mean	0.867	0.133	0.061
	Max	5.55	0.466	0.253
	Min	0.143	0.049	0.017
Slope ratio	Mean	1.41	1.59	0.35
	Max	1.784	2.04	0.42
	Min	1.03	1.29	0.29
Shift [Sampling unit]	Mean	-12.	-13.7	
	Max	-9	-12	
	Min	-14	-16	
False-to-true peak ratio (%)	Mean			22.7
	Max			34.7
	Min			9.4

Table 3.5 a: The results from analyzing all near and distant MFP contributions using the McGill filter on 25 SF_LIB MFP library. Statistically the filtered data show more sharpness and symmetry than the CN_LIB library data.

McGill filter and 40 SF_lib		Peaks representing near MFP contributions from the near MFP library	Peaks representing distant MFP contributions from the distant MFP library	False peaks created from near MFP contributions from the near MFP library
Amplitude [μV]	Mean	157	29.8	27.9
	Max	591.3	100.8	79
	Min	37.7	11.5	10.1
Sharpness [μV/μs]	Mean	1.214	0.167	0.077
	Max	5.553	0.661	0.253
	Min	0.214	0.049	0.024
Slope ratio	Mean	1.39	1.57	0.35
	Max	1.635	2.04	0.41
	Min	1.03	1.24	0.29
Shift [Sampling unit]	Mean	-11.7	-13.5	
	Max	-9	-12	
	Min	-14	-16	
False-to-true peak ratio (%)	Mean			20.4
	Max			30.5
	Min			9.4

Table 3.5 b: The results from analyzing all near and distant MFP contributions using the McGill filter on the 40 SF_LIB MFP library.

ButterWorth filter and 25 SF_lib 500~10k		Peaks representing near MFP contributions from the near MFP library	Peaks representing distant MFP contributions from the distant MFP library	False peaks created from near MFP contributions from the near MFP library
Amplitude [μV]	Mean	105.8	38.9	7.8
	Max	337.8	79.8	21.8
	Min	42.2	22.7	3.6
Sharpness [μV/μs]	Mean	0.418	0.145	0.011
	Max	1.398	0.302	0.033
	Min	0.154	0.075	0.005
Slope ratio	Mean	0.558	0.595	2.85
	Max	0.713	0.668	3.33
	Min	0.443	0.496	2.56
Shift [Sampling unit]	Mean	-0.24	-0.26	
	Max	-0	-0	
	Min	-1	-1	
False-to-true peak ratio (%)	Mean			7.6
	Max			10.5
	Min			4.9

Table 3.5 c: The results from analyzing all near and distant MFP contributions using the 500hz to 10khz band pass Butterworth filter on the 25 SF_LIB MFP library.

Butterworth filter and 40 SF_lib 500~10k		Peaks representing near MFP contributions from the near MFP library	Peaks representing distant MFP contributions from the distant MFP library	False peaks created from near MFP contributions from the near MFP library
Amplitude [μV]	Mean	130.5	43.6	9.3
	Max	337.8	10.4	21.7
	Min	52.5	22.8	4.15
Sharpness [μV/μs]	Mean	0.519	0.163	0.014
	Max	1.398	0.426	0.033
	Min	0.197	0.075	0.006
Slope ratio	Mean	0.548	0.59	2.89
	Max	0.708	0.713	3.33
	Min	0.443	0.479	2.58
Shift [Sampling unit]	Mean	-0.2	-0.26	
	Max	-0	-0	
	Min	-1	-1	
False-to-true peak ratio (%)	Mean			7.3
	Max			10.5
	Min			4.9

Table 3.5 d: The results from analyzing all near and distant MFP contributions using the 500hz to 10khz band pass Butterworth filter on the 40 SF_LIB MFP library.

Butterworth filter and 25 SF_lib 1k~10k		Peaks representing near MFP contributions from the near MFP library	Peaks representing distant MFP contributions from the distant MFP library	False peaks created from near MFP contributions from the near MFP library
Amplitude [μV]	Mean	58.4	17.1	14.4
	Max	224	39.9	54.4
	Min	18.1	7.9	4.3
Sharpness [μV/μs]	Mean	0.311	0.088	0.05
	Max	1.22	0.21	0.187
	Min	0.089	0.036	0.015
Slope ratio	Mean	0.668	0.681	2.55
	Max	0.795	0.845	3.6
	Min	0.54	0.56	2.02
Shift [Sampling unit]	Mean	-1.07	-1.2	
	Max	-0	-0	
	Min	-2	-2	
False-to-true peak ratio (%)	Mean			24.3
	Max			40.4
	Min			18.6

Table 3.5 e: The results from analyzing all near and distant MFP contributions using the 1khz to 10khz band pass Butterworth filter on the 25 SF_LIB MFP library.

Butterworth filter and 40 SF_lib 1k~10k		Peaks representing near MFP contributions from the near MFP library	Peaks representing distant MFP contributions from the distant MFP library	False peaks created from near MFP contributions from the near MFP library
Amplitude [μV]	Mean	74.5	19.7	18.7
	Max	224	57.1	54.3
	Min	23.9	7.9	5.6
Sharpness [μV/μs]	Mean	0.398	0.102	0.064
	Max	1.224	0.31	0.187
	Min	0.12	0.036	0.019
Slope ratio	Mean	0.657	0.682	2.59
	Max	0.783	0.845	3.6
	Min	0.54	0.56	2.05
Shift [Sampling unit]	Mean	-1	-1.2	
	Max	-0	-0	
	Min	-2	-2	
False-to-true peak ratio (%)	Mean			24.7
	Max			40.5
	Min			19.5

Table 3.5 f: The results from analyzing all near and distant MFP contributions using the 1khz to 10khz band pass Butterworth filter on the 40 SF_LIB MFP library.

Butterworth filter and 25 SF_lib 2k~10k		Peaks representing near MFP contributions from the near MFP library	Peaks representing distant MFP contributions from the distant MFP library	False peaks created from near MFP contributions from the near MFP library
Amplitude [μV]	Mean	15.7	2.8	9.8
	Max	83.7	8.7	63.4
	Min	3.0	0	0
Sharpness [μV/μs]	Mean	0.11	0.019	0.066
	Max	0.59	0.059	0.439
	Min	0.019	0.0	0
Slope ratio	Mean	0.644	0.601	2.28
	Max	3.45	0.816	3.8
	Min	0.40	0.0	0
Shift [Sampling unit]	Mean	-3.1	-2.4	
	Max	-2	-0	
	Min	-17	-4	
False-to-true peak ratio (%)	Mean			0.54
	Max			99.6
	Min			0

Table 3.5 g: The results from analyzing all near and distant MFP contributions using the 2khz to 10khz band pass Butterworth filter on the 25 SF_LIB MFP library.

Butterworth filter and 40 SF_lib 2k~10k		Peaks representing near MFP contributions from the near MFP library	Peaks representing distant MFP contributions from the distant MFP library	False peaks created from near MFP contributions from the near MFP library
Amplitude [μV]	Mean	21.3	3.5	13.9
	Max	83.7	14.2	63.4
	Min	4.3	0	2.14
Sharpness [μV/μs]	Mean	0.15	0.024	0.095
	Max	0.59	0.106	0.439
	Min	0.027	0.0	0.012
Slope ratio	Mean	0.653	0.607	2.37
	Max	3.45	0.817	3.82
	Min	0.4	0.0	0.47
Shift [Sampling unit]	Mean	-3	-2.5	
	Max	-2	-0	
	Min	-17	-4	
False-to-true peak ratio (%)	Mean			60
	Max			99.6
	Min			41.6

Table 3.5 h: The results from analyzing all near and distant MFP contributions using the 2khz to 10khz band pass Butterworth filter on the 40 SF_LIB MFP library.

When filtered using the same filter, the CN and SF filtered data, had similar statistical characteristics, except that the SF data had somewhat larger amplitude and sharpness. In general, using the McGill, Acceleration or the wider bandwidth Butterworth filter, near and distant MFP contributions can be differentiated using differences in the slope ratio and sharpness of the detected peaks. True and false peaks can be identified by their distinct slope ratio and amplitude. The amount of temporal shift of the detected peaks may help us decide the correspondence between the detected MFP contributions and the locations of the expected MFP contributions. Therefore, by using suitable thresholds for the detection parameters, near MFP contributions can be detected.

3.8 Detecting Near MFP Contributions in MUPs

3.8.1 Determining Detection Thresholds Using Simulated MUPs

These filters were then applied to the created MUP libraries to determine optimised feature value thresholds for the detection of individual MFP contributions. Accurately

measuring neuromuscular jitter is dependent on the ability to consistently and accurately detect individual MFP contributions.

The thresholds of the three detection parameters, amplitude, sharpness and slope ratio, were decided by considering the false and missed detection rates. The optimal thresholds should generate a minimum false and missed detection rate. Actually, it is almost impossible that no false and no missed peaks occur in an actual detection. But either or both of them should be as small as possible. For measuring neuromuscular jitter, false peaks are more unfavourable than missed peaks. So when adjusting the thresholds, if a decrease of false detection rate lead to an increase in missed detection rate, a low false detection rate was considered first. For an acceptable false detection rate, when the ratio of missed detection rate increase to false detection rate decrease was more than 1, the false detection rate was fixed and the corresponding thresholds that have the minimum missed detection rate were defined as the optimal thresholds. Table 3.6 shows the optimal detection parameters for using the McGill and Acceleration filters and the Butterworth filter for detecting near MFP contributions.

	McGill/Accel				Butterworth				
Threshold	sharpness	peak	Symmetry	Symmetry	sharpness	peak	Symmetry		
CN	0.078	0.004	low 0.5	high 0.7	0.06	0.004	low 0.5	high 0.7	cut 1.2
SF	0.078	0.004	low 0.3	high 0.4	0.06	0.004	low 0.3	high 0.4	cut 1.5

Table 3.6: MFP contribution detection thresholds for the McGill, Acceleration and Butterworth filers.

The logic of using high and low symmetric value here is, if we have a peak that is very sharp, then we can use the low level of symmetric threshold. If a peak is not very sharp, but if we use several data points close to the peak top to calculate the sharpness again and this sharpness satisfy the sharpness threshold, then it must also satisfy the high level of symmetric threshold. Table 3.6 shows the optimal detection thresholds for the different filters. When analyzing the detection results, usually we have two types of error rates: false and missed detection rates. In our case, most false peaks were not generated by the filters, but instead were often the result of a ‘large’ distant MFP or a superposition of distant MFPs. Missed peaks occurred for various reasons. Most of them came from

temporal overlap of near MFP contributions. In fact, every detection filter had a minimum time resolution. When two or more MFP contributions were so close that their peak intervals were shorter than the time resolution of the filter, one or more near MFP contributions was missed. In addition, false peaks may also caused near MFP contributions to be missed. If a near MFP contribution with relatively small amplitude followed another MFP contribution with large amplitude, then the false peak that appeared in the tail of the detected large MFP contribution sometimes covered the detected contribution of the following small MFP and caused the small contribution to be missed.

Effects of noise are complicated. High levels of noise can lead to both false and missed peaks. Therefore, a narrow passband bandwidth for the detection filters was chosen in order to reduce noise to the maximum extent. In addition, increasing the levels of the detection thresholds was the major means for reducing the effects of noise. However, this lead to an increase of the missed detection rate while decreasing the false detection rate.

Compared with the McGill filter, the Acceleration had similar results with regard to false and missed peaks. In addition, the detection thresholds for the Acceleration filter were determined by the same method. In general, the threshold combinations that resulted in a small false detection rate and a relatively small missed detection rate are expected to be optimal for measuring neuromuscular jitter. A major limitation in the ability to detect fibre contributions is the temporal overlap of individual MFPs. Temporasl overlap results in some near MFP contributions being missed so that any detection scheme will underestimate the true number of contributions. Although temporal overlap can be identified to some extent by analysing the stability of a peak shape across an ensemble of detected individual contributions, it is a difficult task to automatically detect such temporally close MFP contributions. In addition, overlap also makes the analysis more difficult.

3.9 Discussion of Filter Chosen

Using SF EMG data to measure neuromuscular jitter and fibre density is the current clinical standard technique. SF MUPs are acquired using the combination of a SF

electrode and a band pass filter with cut-off frequencies of 500 Hz and 10 kHz, and usually consist of one or a few individual MFPs. In fact, the accuracy of jitter and fibre density measurements is dependent on the extent to which individual MFP contributions can be correctly detected. So far, the performance of using the McGill filter to detect near MFP contributions in CN MUPs has been analyzed. However, it was also necessary to evaluate the performance of the McGill filter using SF MUPs, and to compare the detection results with the clinical standard technique. Therefore, contrast experiments were implemented between the Acceleration filter and the bandpass Butterworth filter with cut-off frequencies of 500 Hz and 10 kHz using simulated CN and SF MUPs.

Simulated CN and SF MUPs were established by the same conditions, except for using different electrodes. Here we first used the different filters to detect near MFP contributions with one MUP composed of two MFPs, near MFP contributions were defined as detected peaks with a stable shape. We show the results intuitively in a plot and then statistically. The detection results were evaluated using the same criteria presented in section 3.8. Figures 3.8, 3.9 and 3.10 show examples of MUPs, composed of two MFP contributions with different time shifts, processed by different filters.

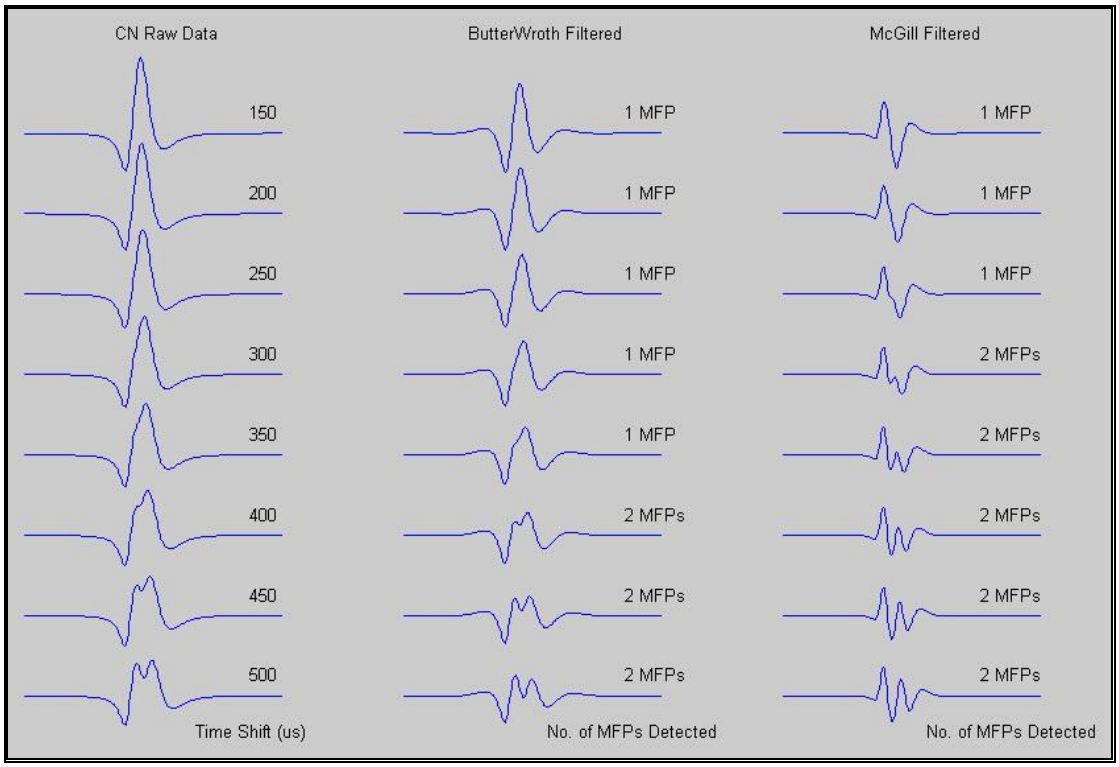

Figure 3.8: Example of detecting near MFP contributions to CN MUPs. On the left are raw CN MUPs composed of two MFPs with different time shifts, in the middle near MFP contributions are detected using a Butterworth bandpass filter, and on the left are the results of McGill filtering and MFP detection.

We can see the McGill filter has better time resolution than the Butterworth filter. Under the same conditions with a 300 μs time shift the McGill Filter allows the two MFP contributions to be detected, while the Butterworth filter requires a time shift of 400 μs before both MFP contributions can be detected.

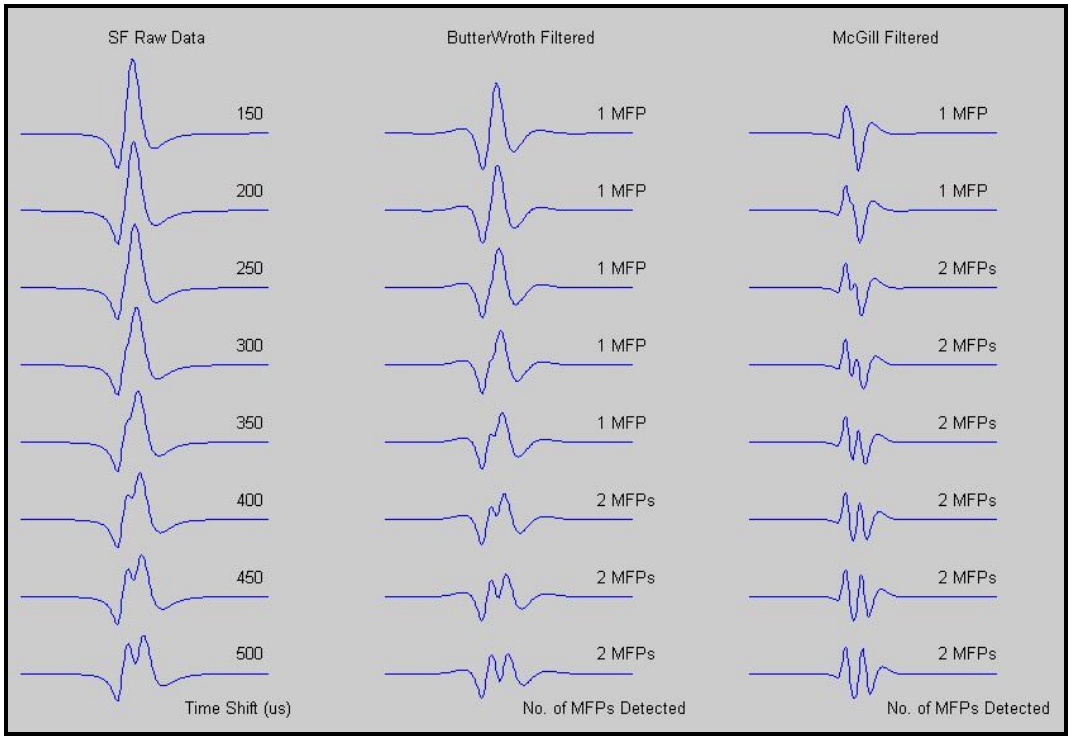

Figure 3.9: Example for detecting near MFP contributions to SF MUPs. On the left are raw SF MUPs composed of two MFP contributions with different time shifts, in the middle near MFP contributions are detected using Butterworth bandpass filter, and on the left results using the McGill filter are shown.

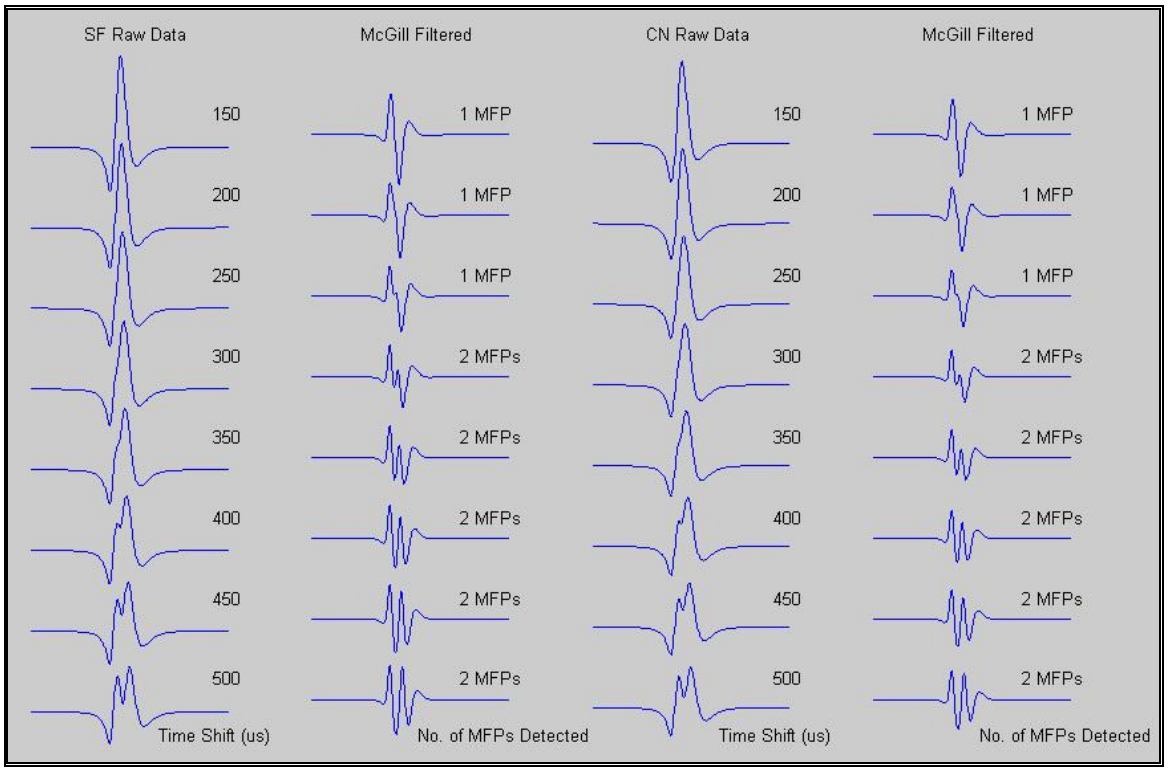

Figure 3.10: Example for detecting near MFP contributions to SF and CN MUPs using the McGill filter. On the left are raw SF MUPs composed of two MFP contributions with different time shifts and the McGill filtered MFP detection result, and on the left are CN MUPs composed of the corresponding MFP contributions and McGill filtered MFP detection results.

Compared with the conventional technique, the McGill filter has a better detection ability as shown in Figures 3.8, 3.9 and 3.10. In fact, it works very well not only for SF MUPs but also for CN MUPs.

In order to get a more accurate estimate of how well these filters work, MUPs were generated with two near MFP contributions randomly selected from the MFP libraries. The selected MFPs were combined with a fixed amount of time shift between them to create each MUP and the created MUPs were processed by the different filters and the MFP detection routines were applied to obtain statistical data. Tables 3.7 and 3.8 display the results.

time shift (micro-sec)	Accel 25	Accel 40	McGill 25	McGill 40	ButtW 25	ButtW 40
250	28.3	44.8	29.2	47	5.5	8.9
300	63.7	85	72.5	87.3	15.5	27.4
350	81.5	90.9	84	89.2	31.1	52
400	89.5	91.9	90.3	93.8	56.1	69.5
450	96.6	98.7	95.3	98.1	65.4	74.6
500	98.8	99.8	99.5	100	73.6	78.1
550	100	100	100		80.9	86.1
600					87.4	95.3
650					94.3	99
700					98.4	100
750					99.7	
800					100	

Table 3.7: MFP detection accuracies for 1000 CN MUPs, composed of two randomly selected MFPs with fixed time shifts using different filtering and selecting from different MFP libraries.

We can see that for both the 25CN and 40 CN libraries, the Acceleration and McGill filter out performed the Butterworth filter. At first it was expected that the Acceleration filter would have better performance than the McGill filter, but statistically this was not the case. Tthe computation cost of the Acceleration filter is much higher than McGill filter, so we chose the Butterworth and McGill filters for further study.

time shift	McGill SF 25lib		McGill SF 40lib		Butterworth SF 25lib		Butterworth SF 40lib	
	same	Random	Same	random	same	random	same	random
250	35.3	44.7	55.8	54.6	0	2.7	0	6.4
300	84.4	74	94.1	81.5	11.6	11.1	19.6	18.5
350	100	83.8	100	83.7	45.1	37.8	67.7	51.1
400		88.8		89.1	84.97	63.2	93.14	67.9
450		92.7		95.8	100	74.1	100	77.7
500		98.2		98.8		86.2		89.6
550		99.7		99.1		94.3		95.1
600		100		100		95.7		98.5
650						99.2		99.6
700						99.9		99.9
750						100		100

Table 3.8: MFP detection accuracies for 1000 SF MUPs, composed of two randomly selected MFPs with fixed time shifts using different filtering and selecting from different MFP libraries.

We can see that for both the 25SF and 40SF library, the McGill filter out performed the Butterworth filter. The “same” column using the same SF MFP twice to remove different MFP overlap, so we can have a no overlap estimate.

McGill	correct	FALSE	miss	avg IPI		correct	FALSE	Miss	avg IPI
SF 0	89.7	4.7	6.6	524	CN 0	86.3	5.2	8.5	519
	89.9	4.9	6.2	525		86.9	5	8.1	514
	89.1	5.1	6.8	528		85.8	4.9	9.3	516
2.5	86.5	7.1	6.4	522	2.5	87.6	5.7	6.7	520
	87.3	7.6	5.1	515		86.3	5.7	8	511
	88.7	6.1	5.2	524		85.2	6.7	8.1	516
5	84.6	9.3	6.1	522	5	85.5	7.4	7.1	520
	83.9	10.7	5.4	541		84.7	7.6	7.7	508
	85.4	9.2	5.4	522		84.7	7.9	7.4	522

Table 3.9: MFP detection accuracies for 1000 CN MUPs, composed of two randomly selected MFPs with fixed time shifts and three distant MFP contributions using McGill filtering.

The rate at which the correct number of MFP contributions is reported as well as the rate at which extra or missed contributions were detected. The average interval between the two near MFP contributions or the inter-potential-interval (IPI) is also reported.

In this section, detection thresholds were determined and the detection results were analysed and discussed. Three filters were applied to detect near MFP contributions to

MUPs. Based on analyzing simulated MUPs it can be concluded that the McGill, Acceleration and Butterworth filters are all powerful techniques for detecting major fibre contributions to MUPs, and are able to consistently detect near MFP contributions in MUPs. Accurate detection of near MFP contributions establishes the essential conditions for measuring neuromuscular jitter discussed in the next chapter.

Comparing the McGill, Acceleration and Butterworth filters, it can be concluded that they all have very similar detection results. For the McGill and Acceleration filters, their characteristics are also essentially alike and the major difference between them is merely that the Acceleration filter has a better ability to inhibit high frequency noise. The Acceleration and McGill filters have similar time resolutions. But the computation cost of the Acceleration filer is much greater than the McGill filer. Therefore, the McGill filter was chosen as the tool of detecting individual MFP contributions for measuring neuromuscular jitter.

And also we can see that by applying these filters to CN and SF signals we get very close result. Usually SF signals are more easily to detect, so the correct rates are a little bit higher than CN.

Chapter 4 A Method for Neuromuscular Jitter Measurement

4.1 Introduction

In previous chapters we have discussed the definition of neuromuscular jitter and technology that can be used to detect MFP contributions for the measurement of neuromuscular jitter. However, to measure jitter in MUPs, not only MFPs, but individual MFP pairs have to be found. Furthermore, due to the superposition of MUPs from different MUs, detected MFP contributions to a detected MUP waveform may not have been created by a single MU. Therefore, a method to remove these overlapped signals is required. Moreover, due to biological variations and noise interference, the waveform of each MUP belonging to a MUPT is not exactly identical. Therefore, the detection results across the MUPs of a MUPT may contain false or missed individual MUP contributions. Typical features of detected contributions from different MUPs in the same MUPT therefore have to be found in order to exclude incorrect detection results. In addition, measurement of jitter should be with respect to a specific fibre pair, but often more than two near MFP contributions may be detected. Consequently, specific individual MFP pairs have to be identified in order to measure their IPIs across a set of firings of a MU. This chapter deals with the steps of how to identify specific individual MFP pairs in a series of filtered MUPs and results under different filters.

With regard to the measurement of jitter, blocking is also an important factor. Blocking is referred to as a particular fibre failing to fire at some time during a train of MU discharges. Blocking represents a failure of the NMJ, and is very important for clinical interpretation of jitter measurements. As jitter increases, blocking may occur. In particular, blocking almost always occurs when MCD values exceed 100 μs [33]. Normal jitter values range between 10 and 50 μs, and a time resolution of at least 1 μs is usually expected. However, MUP data used in this research were sampled at 31.25 kHz, and thus the sampling time interval is 32 μs. Consequently, a suitable interpolation technique must be applied in order to obtain more accurate measurement results and to satisfy the time resolution requirement.

For evaluating the accuracy of the jitter measurement techniques, simulated EMG signals and MUP data with known jitter values were implemented. Different jitter measurement results using the same method with CN and SF MUPs, with McGill and Butterworth filtering were compared. Finally, the measurement techniques were evaluated and relevant problems are discussed.

Based on expected jitter values, simulated MUPTs with a signal-to-noise ratio of 20 dB were randomly created. Individual MFP pairs were identified in these MUPTs using nearest neighbour clustering and minimum spanning tree algorithms, jitter and blocking was measured for every MUPT whose MUPs contain available individual MFP pairs and errors in the measurements were calculated. In addition, the developed algorithm was verified using four types of simulated EMG signals built randomly.

There are four major sections in this jitter measurement method and each one contains a number of steps:

1. Select isolated MUPs.

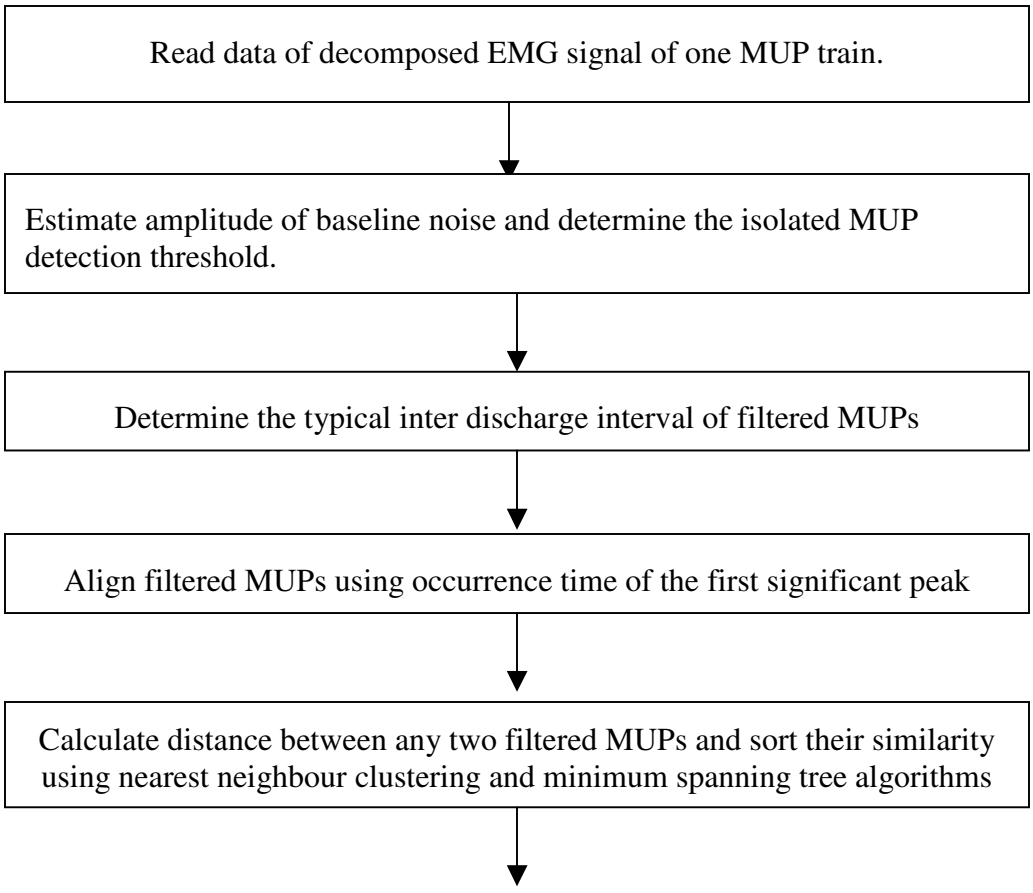

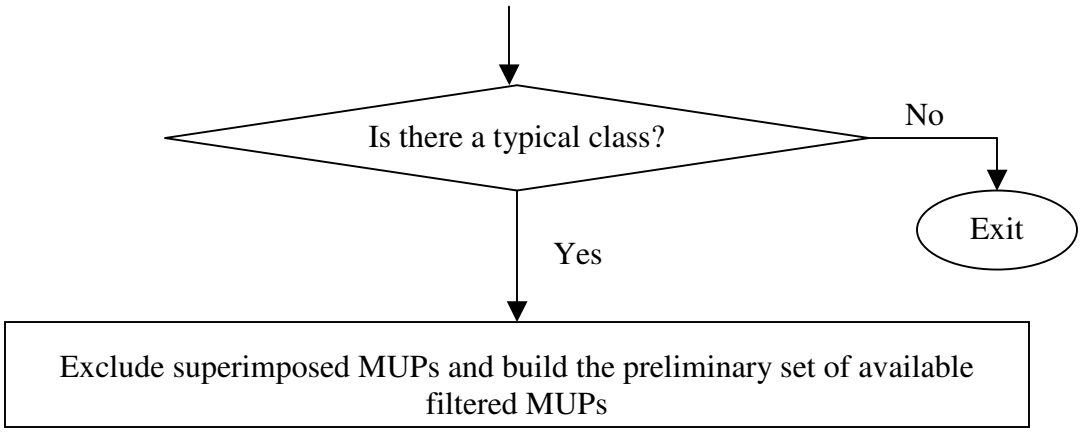

2. Select individual MFPs.

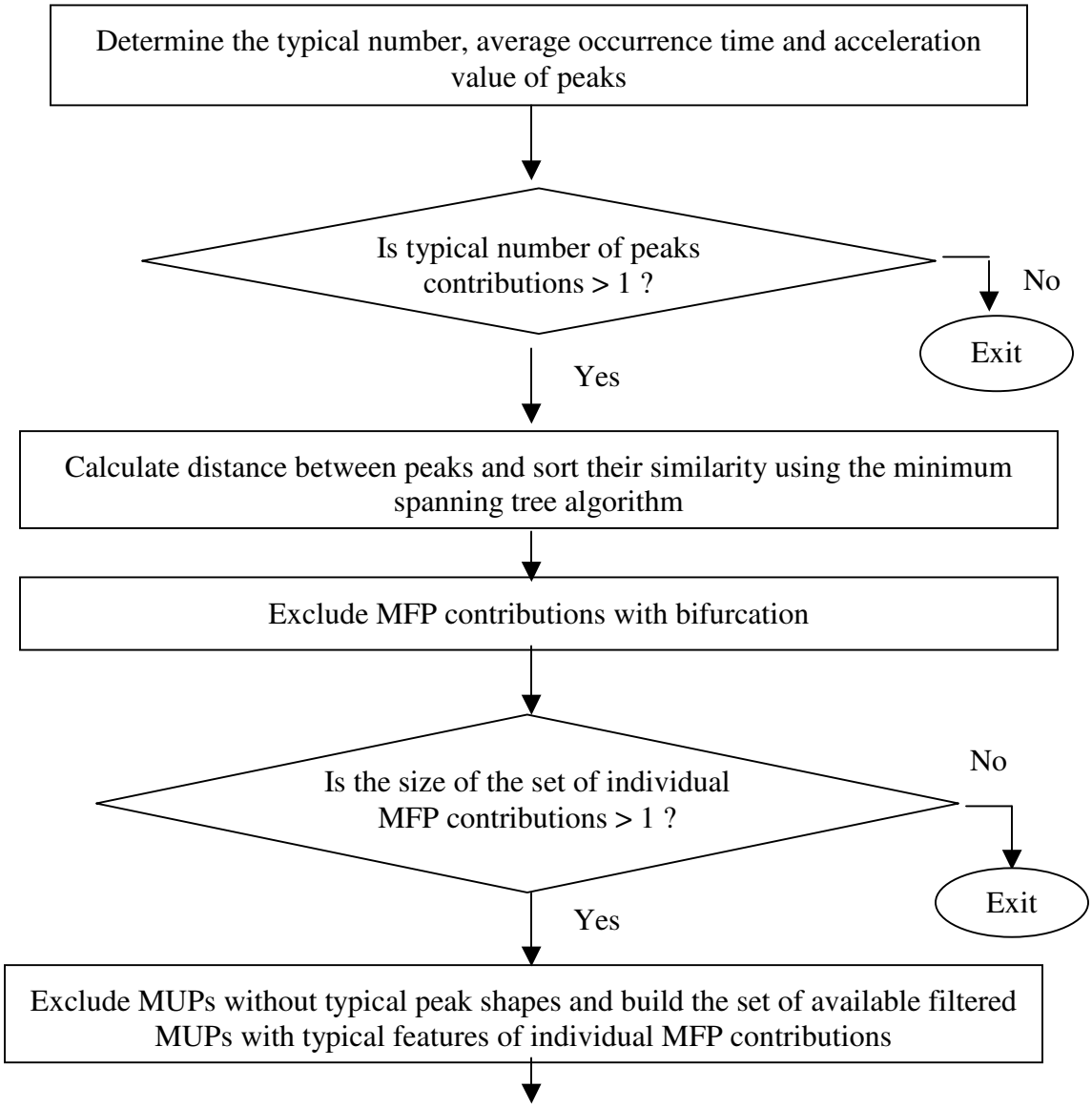

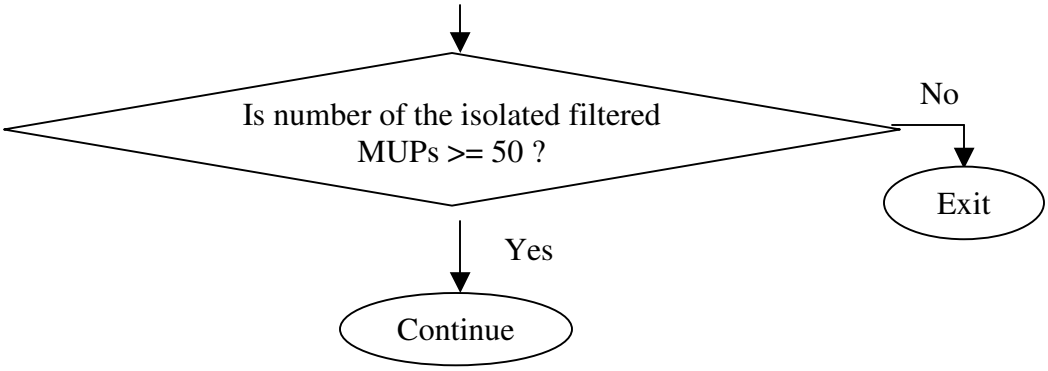

3. Select pairs of individual MFPs.

Identify pairs of individual MFPs by the occurrence order of the corresponding MFP contributions in the set of isolated filtered MUPs

4. Calculate jitter and blocking.

Calculate jitter for each unique pair of individual MFP contributions

4.2 Selecting Isolated MUPs

For the ideal circumstance, all results for detecting individual MFP contributions in different MUPs of the same MUPT should be exactly consistent, and individual MFP pairs can be simply identified according to the occurrence order of the corresponding detected contributions in the filtered MUPs. In fact, however, the detected results usually vary. For instance, superposition of individual MUPs from different MUs may generate more individual MFP contributions, and strong noise may lead to false or missed MFP contributions. Figure 4.1 shows the result of classification of a MUP train. We can't use all MUPs here to measure jitter because of superpositions.

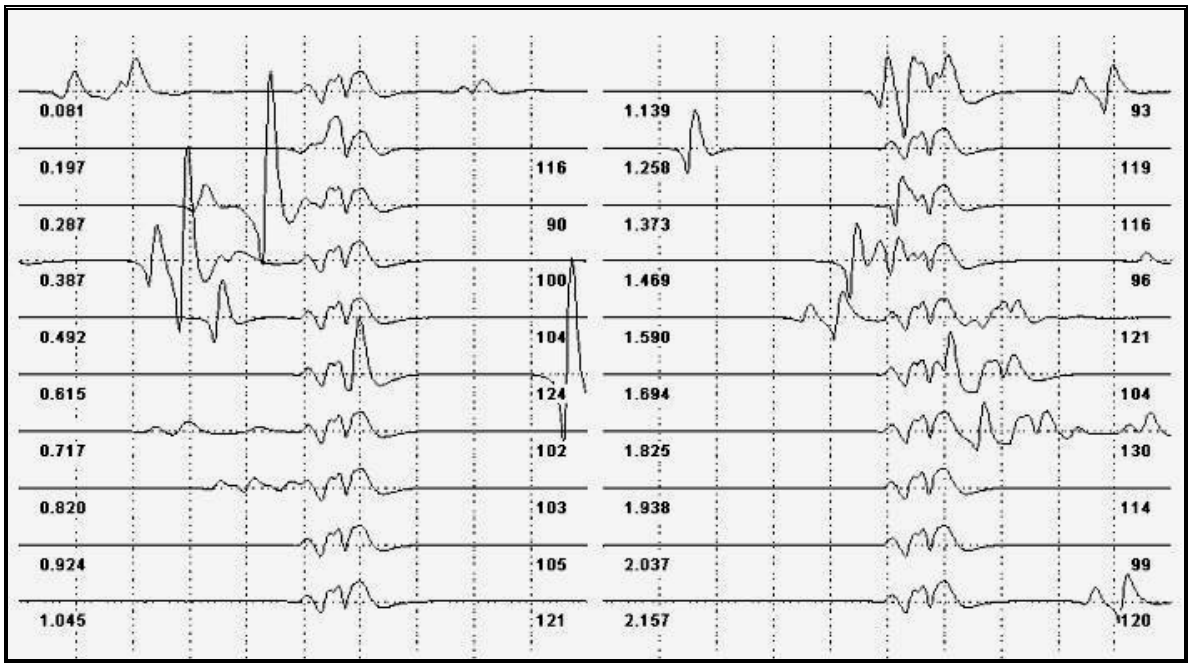

Figure 4.1: EMG Signal decomposition result: one MUP train.

The minimum spanning tree (MST) was used to select isolated MUPs, there are commonly two MST algorithms: Prim's algorithm and Kruskal's algorithm. Kruskal's algorithm was choosen. The basic step is to sort all the distances between any two MUPs in one MUP train and choose the first thirty to fifty most similar MUPs to calculate the mean and variance of the inter-MUP distances. Based on experimental tests, if the distance is bigger than 2.4 to 2.9 times the variance plus the mean value, we mark the MUP as not isolated (i.e. as a superimposed waveform). The threshold selected dynamically adjusts with the amount of jitter. As the jitter increases the variance of the distances will also increase, so the threshold will be higher. This gives better results then a fixed threshold algorithm. When the MST code is implemented in MatLab, it takes about 30 minutes to process a normal contraction. The code was then optimized and implemented in C++ and now takes only 30 seconds to process the same contraction data. Figure 4.2 shows the sorted distance in one MUP train and a certain thresold can be set to select isolated MUPs.

To reduce the effect of jitter, seven distances are calculated by shifting the second filtered MUP for each similarity measurement and the minimum distance is selected. Using the nearest neighbour clustering and MST tree algorithms the similarity of the

filtered MUPs are sorted based on their distances. The detection thresholds of superimposed MUPs are determined based on the mean and standard deviation of the distances. The typical class, the biggest MUP group with similar shape, can then be found and most of the superimposed MUPs can be excluded. Using the typical class, the preliminary set of the available filtered MUPs is set up.

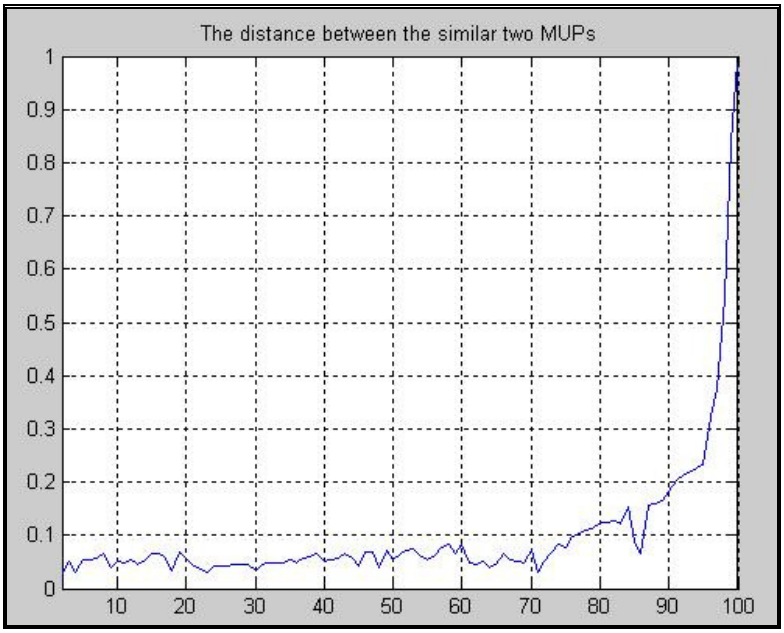

Figure 4.2: Distance between two MUPs in one MUP train. If the distance is greater than a ceterain thershold, the MUP is assumed to be superimposed and won't be used to calculate jitter.

Figure 4.3 (a) and (b) shows the result of applying the MST algorithm to a MUP train. This figure demonstrates that superimposed MUPs have been successfully seperated from isolated MUPs.

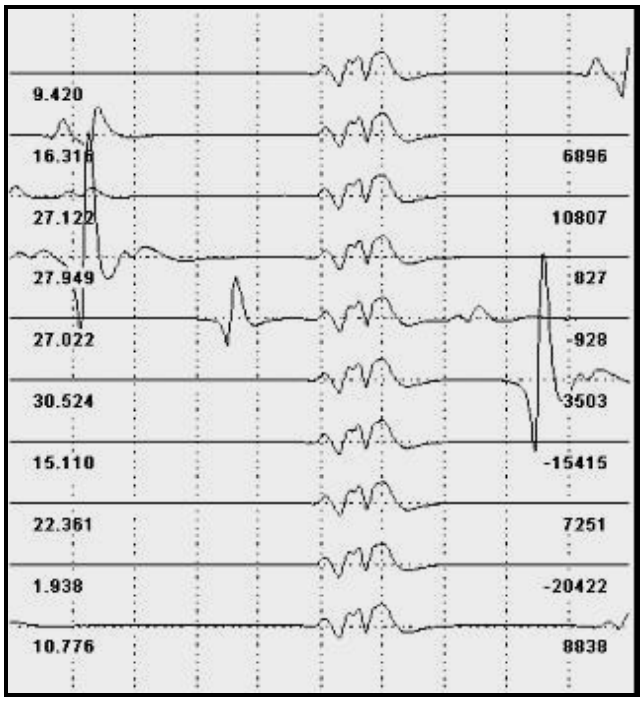

Figure 4.3 a: Isolated MUPs that can be further processed to calculate jitter.

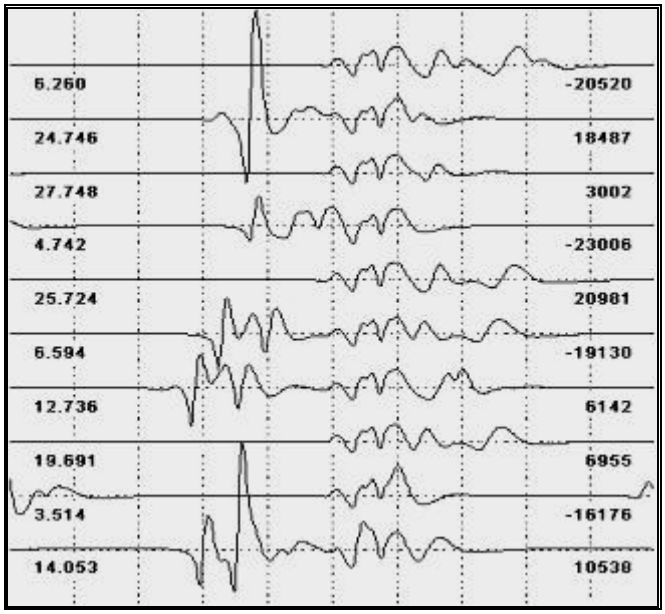

Figure 4.3 b: Superimposed MUPs excluded from jitter measurement calculations.

Table 4.1 shows the results of using the mean distance plus 2.4 times the variance as the threshold for selecting isolated MUPs, for different jitter values.

jitter50		# of superimposed MUPs included	# of Isolated MUPs missed	Total # of Errors	Error Rate %
train1	189	0	9	9	4.8
train2	272	1	15	16	5.9
train3	153	0	12	12	7.8
train4	122	0	9	9	7.4
train5	170	0	7	8	4.7
jitter100		# of superimposed MUPs included	# of Isolated MUPs missed	Total # of Errors	Error Rate %
train1	172	0	10	10	5.8
train2	265	1	13	14	5.3
train3	125	0	9	9	7.2
train4	132	0	7	7	5.3
train5	156	0	10	10	6.4
jitter150		# of superimposed MUPs included	# of Isolated MUPs missed	Total # of Errors	Error Rate %
train1	150	0	10	10	6.7
train2	220	0	13	13	5.9
train3	125	0	12	12	9.6
train4	153	0	13	13	8.5
train5	202	1	13	14	6.9

Table 4.1: Use of the MST and threshold method to select isolated MUPs; by excluding less than 10% of the isolated MUPs we can get very low inclusion of superimposed MUPs for further jitter measurement.

4.3 Choosing MFPs for Jitter Calculation

This MST method can also be applied to MFPs to exclude bifurcated MFPs. Detected MFP contributions may not result from individual MFPs due to the superposition of individual MFPs from the same MU. Particularly, this may be more serious for detected MUPs with high jitter. Therefore, the shapes of detected individual MFP contributions have to be analysed and the detected peaks from individual MFPs should be stable, smooth and have no bifurcation across the ensemble of MUPs of a MUPT. Finally, if individual MFPs can be identified, MFP pairs can be selected and neuromuscular jitter measured.

To reduce the effect of noise, the amplitude of the baseline noise was estimated in order to determine detection thresholds for peaks and near MFP contributions. According

to the typical occurrence time of pre-detected contributions, the significant detection range of filtered MUPs, which is used to compare similarity between any two MUPs, can be determined. To accurately measure similarity, the first positive peaks in every filtered MUP are aligned at the same position.

The typical number, average occurrence time and amplitude of near MFP contributions are determined based on the preliminary set of available filtered MUPs. The typical number is the number of detected contributions that appear most frequently in the set. Average occurrence time and amplitude are then calculated based on initial estimates of jitter and amplitude variability. Here, the average occurrence times are determined in two steps. First, the mean and standard deviation of every contribution's occurrence time are calculated using the available filtered MUPs with the typical number of detected contributions. If the deviation is greater than 128 μs, the detected contributions with occurrence times greater than 1.65 standard deviations away from the mean (about 10% probability) are excluded. The mean of every contribution's occurrence time is then recalculated and the results are thought of as the average occurrence time of the corresponding contributions. Independent of any measured standard deviation, if any contribution's occurrence time is farther than 320 μs from the corresponding average occurrence time, the detected contribution is excluded. If the amplitude of a detected contribution is greater than 1.5 times or smaller than half the average amplitude, the contribution is also discarded. In addition, for accurately measuring jitter and blocking, the detected contributions are also excluded in the following two cases. First, if the average amplitude of the detected contributions is around the detection threshold, the contribution is excluded in order to prevent noise interference. Second, if the average interval between two detected contributions is within 480 μs and the average amplitude of the second one is smaller than that of the first one, the second one is also discarded in order to prevent errors from the effect of false peaks.

The MUPs selected for jitter measurement should contain contributions with occurrence times and amplitudes similar to the average occurrence time and amplitude of the corresponding contributions. If the typical number of the detected contributions is two or more and the number of the available MUPs is greater than fifty, it is possible to

use the available filtered MUPs to measure neuromuscular jitter. However, features of the detected peaks that represent near MFP contributions should be analysed further to assure that the detected contributions are in fact created by individual MFPs. The MST algorithm is used again to measure the similarity between any two peaks within each corresponding detected MFP contribution. Here, to reduce the effect of noise and low sampling rate, three distances are calculated by shifting one of the peaks and the minimum distance is used to represent the similarity between any two peaks. For each contribution, if there is only a typical class, then the detected contributions can be considered as individual MFP contributions. Otherwise, the detected peaks have bifurcation and the corresponding contributions may result from superposition of more than one individual MFP and are not used for jitter measurement. After individual MFP contributions are identified, peaks that are away from the typical shape are discarded and the corresponding MUPs are also excluded in order to assure the accuracy of the jitter measurement (distortion of the peak usually results from the superposition of MUPs or the effect of large noise). Finally, the remaining MUPs are the filtered MUPs available for jitter measurement and their number should be greater than fifty.

After the available filtered MUPs are obtained, the individual MFPs are marked simply by their occurrence order, and individual MFP pairs are selected by their occurrence order number. Examples of selecting MFP pairs were shown bellow.

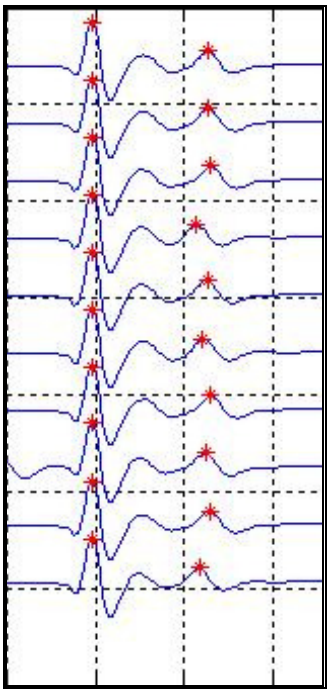

Figure 4.4: Example of a pair of MFP contributions.

Based on the average occurrence times and amplitudes of individual MFP contributions, blocking is identified and percent blocking is calculated. Based on the jitter value and the average occurrence time of the corresponding contribution, the positive peak is searched for in every filtered MUP. If no matched positive peak is found, a blocking is identified. The percent blocking is calculated by the ratio of the number of detected blockings to the total number of the filtered MUPs.

4.4 Measuring Neuromuscular Jitter in MUPs

Jitter measurement requires time resolution of approximately 1 μs. To meet the requirement of neuromuscular jitter measurement, an interpolation technique is used for available MUP data, which are sampled using a sampling rate of 31.25 kHz, a time resolution of 32 μs. Figure 4.6 illustrates an example of the necessity of interpolation – Cubic spline [8]. The left figure shows a waveform with a high sampling rate (937.5 kHz), and the * represents the expected occurrence time of the peak. In the right figure, the same waveform, sampled with a sampling rate of 31.25 kHz is plotted using a solid line, and the dotted line represents the interpolated result. Compared to the peak'

occurrence time without interpolation (marked by ‘o’), the occurrence time of the interpolated peak (marked by ‘*’) clearly has a smaller error.

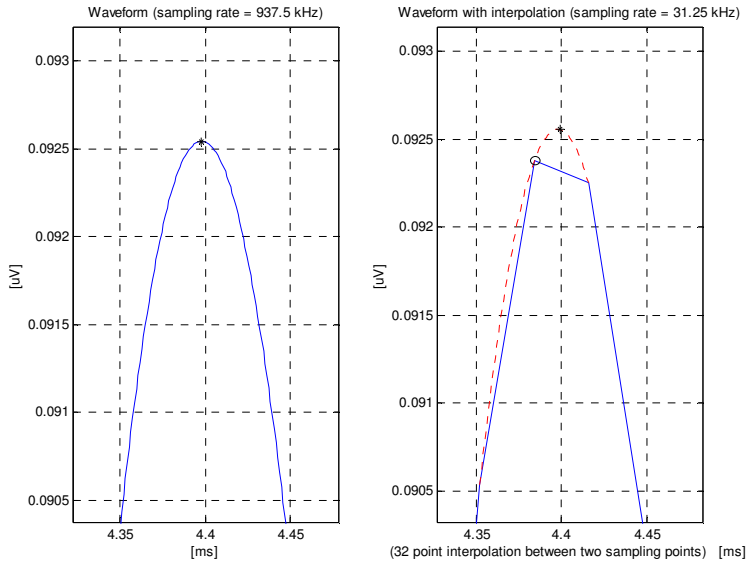

Figure 4.4: An example of the necessity for interpolation. In the left figure, the waveform was sampled at 937.5 kHz, and the maximum possible error of occurrence time of the peak (marked by *) is only 0.535 μs. In the right figure, the solid line represents the waveform sampled at 31.25 kHz, and its top (marked by ‘o’) may have an error of up to 16 μs. The dotted line is the result of a 32-point interpolation between the two sampling points around the peak, and the error of the interpolated top (marked by ‘*’) is reduced to an average 0.57 μs. [8]

Compared with other interpolation methods, the Cubic spline is implemented easily and the interpolation results are satisfactory.

After pairs of individual MFP pairs are identified, neuromuscular jitter is calculated using the MCD statistic. The application of interpolation can assure sufficient temporal measurement precision. To calculate the jitter of a MFP pair, at least 50 MUPs are required [20]. Jitter measurements were made using synthetic MUPTs, that modelled signals detected using CN and SF electrodes during voluntary muscle contraction. The use of Butterworth and McGill filtering were also compared. Jitter values were calculated in all MUPTs that contained individual MFP contributions. In addition, percent blocking was also measured.

4.5 Jitter measurement with simulated EMG

To verify the validity of the algorithm, jitter measurements were implemented using simulated EMG signals. Four simulated EMG signals were created based on an expected jitter value and a signal-to-noise ratio of 20dB. For each signal, detection using a CN electrode and a 5% MVC level of contraction were simulated. The expected jitter values were 25μs, 50μs, 75μs and 150μs. They represent normal, critical, abnormal and seriously abnormal jitter, respectively. The expected percent blocking was zero for all simulated signals. It should be indicated that, except for the specific requirements, the simulated EMG signals were created randomly. Each simulated EMG signal was decomposed into MUPTs. Near MFP contributions to the MUPs were then detected and individual MFP pairs were identified in each MUPT. Finally, neuromuscular jitter and percent blocking were measured in the MUPTs containing individual MFP pairs. Tables 4.2 to 4.5 indicate the constitution of the four simulated EMG signals and the results of the identification of individual MFP pairs and measurement of neuromuscular jitter, respectively. Trains with less than 100 MUPs were excluded from jitter calculation.

EMG name: run025	Expected jitter value = 25 μs			
Number of trains: 4	MUPT1	MUPT2	MUPT3	MUPT4
Number of MUPs	175	180	157	163
Number of near MFP contributions	2	2	3	1
Number of available filtered MUPs	150	154	138	
Number of available MFP pairs	1	1	3	0
Measured jitter [μs]: MCD	24 μs	26 μs	19/23/23 μs	

Table 4.2: The constitution of the first simulated EMG signal and the results of MFP pair identification and jitter measurement.

EMG name: run050	Expected jitter value = 50μs			
Number of trains: 4	MUPT1	MUPT2	MUPT3	MUPT4
Number of MUPs	193	185	191	174
Number of near MFP contributions	1	2	2	4
Number of available filtered MUPs		162	172	153
Number of available MFP pairs		1	1	1
Measured jitter [μs]: MCD		52 μs	48 μs	47 μs

Table 4.3: The constitution of the second simulated EMG signal and the results of MFP pair identification and jitter measurement.

EMG name: run075	Expected jitter value = 75 μs			
Number of trains: 4	MUPT1	MUPT2	MUPT3	MUPT4
Number of MUPs	183	165	175	179
Number of near MFP contributions	2	0	3	2
Number of available filtered MUPs	161		149	153
Number of available MFP pairs	1		3	1
Measured jitter [μs]: MCD	74 μs		68/73/72 μs	73 μs

Table 4.4: The constitution of the third simulated EMG signal and the results of MFP pair identification and jitter measurement

EMG name: run150	Expected jitter value = 150 μs			
Number of trains: 4	MUPT1	MUPT2	MUPT3	MUPT4
Number of MUPs	169	176	191	178
Number of near MFP contributions	2	1	1	3
Number of available filtered MUPs	148	157	162	148
Number of available MFP pairs	1			1
Measured jitter [μs]: MCD12	134 μs			123 μs

Table 4.5: The constitution of the fourth simulated EMG signal and the results of MFP pair identification and jitter measurement.

As shown in Tables 4.2 and 4.5, there are certain differences between some measurement results and the expected jitter values. These may result from differences between the actual and modelled or expected jitter values. In general, based on the studies of simulated EMG signals, it can be concluded that the results of the jitter measurements can essentially represent the expected jitter values and that the measurement errors are acceptable. We applied the same set of data and same method, only exchanged the McGill filter with a Butterworth filter. We only get one set of results from this analysis, which is listed below:

EMG name: run025	Expected jitter value = 25 μs			
Number of trains: 4	MUPT1	MUPT2	MUPT3	MUPT4

Number of MUPs	140		147	163
Number of near MFP contributions	1		2	1
Number of available filtered MUPs			120	
Number of available MFP pairs			1	
Measured jitter [μs]: MCD			25 μs	

Table 4.6: The result of using a Butterworth filter for jitter measurement. It shows it is very difficult to find MFP pairs under Butterworth filtered data.

The method was also applied to SF EMG data and test results show it works well.

EMG name: runSF025	Expected jitter value = 25 μs			
Number of trains: 4	MUPT1	MUPT2	MUPT3	MUPT4
Number of MUPs	134	178	157	163
Number of near MFP contributions	2	2	2	1
Number of available filtered MUPs		155	138	
Number of available MFP pairs		1	1	
Measured jitter [μs]: MCD		26 μs	27 μs	

EMG name: runSF050	Expected jitter value = 50μs			
Number of trains: 5	MUPT1	MUPT2	MUPT3	MUPT4
Number of MUPs	168	175	170	171
Number of near MFP contributions	2	1	2	2
Number of available filtered MUPs	143		162	156
Number of available MFP pairs	1		1	1
Measured jitter [μs]: MCD	54		50 μs	52 μs

EMG name: runSF075	Expected jitter value = 75 μs			
Number of trains: 4	MUPT1	MUPT2	MUPT3	MUPT4
Number of MUPs	160	146	167	159
Number of near MFP contributions	2	1	2	2
Number of available filtered MUPs	146		160	143
Number of available MFP pairs	1		1	1
Measured jitter [μs]: MCD	76 μs		75 μs	78 μs

EMG name: run150	Expected jitter value = 150 μs			
Number of trains: 4	MUPT1	MUPT2	MUPT3	MUPT4
Number of MUPs	176	156	161	172
Number of near MFP contributions	2	1	2	3
Number of available filtered MUPs	149		134	153
Number of available MFP pairs	1		0	1
Measured jitter [μs]: MCD12	154 μs			157 μs

Table 4.7: The constitution of simulated SF EMG signals and the results of MFP pair identification and jitter measurement.

To have a better understanding of the method, we also applied a Butterworth filter to the same set of data and the results are listed below:

EMG name: runSF050	Expected jitter value = 50μs			
Number of trains: 4	MUPT1	MUPT2	MUPT3	MUPT4
Number of MUPs	149	172	155	170
Number of near MFP contributions	2	1	2	2
Number of available filtered MUPs	134		145	153
Number of available MFP pairs	0		1	0
Measured jitter [μs]: MCD			51 μs	

EMG name: runSF075	Expected jitter value = 75 μs			
Number of trains: 4	MUPT1	MUPT2	MUPT3	MUPT4
Number of MUPs	160	146	167	155
Number of near MFP contributions	1	1	1	2
Number of available filtered MUPs				145
Number of available MFP pairs				1
Measured jitter [μs]: MCD				76 μs

Table 4.8: The constitution of simulated SF EMG signals and the results of MFP pair identification and jitter measurement using a Butterworth filter. Though it is difficult to find MFP pairs using Butterworth filtered data, the jitter values are close to when using McGill filter.

There were 24 groups of SF and CN data generated to compare the different results when using the McGill and Butterworth filter. Out of 57 CN MUAP trains we can get 49

MFP pairs to calculate jitter values when using McGill filer, while when using a Butterworth filter we only get eight pairs. With SF EMG data, out of 57 SF MUAP trains we can get 40 MFP pairs to calculate jitter, but with Butterworth filtered data we only get six MFP pairs. Though the result of jitter values using traditional the Butterworth filter are close to the McGill filtered results, it is much more efficient to use McGill filtered data.

4.6 Discussion

In general, the proposed algorithm demonstrated an acceptable performance, which was more efficient and accurate than previous works, and which can consistently measure jitter in a variety of EMG signals. So far, the performance of the measurement algorithm has been examined using simulated CN and SF MUPs. We also compared the same method but using a Butterworth filter instead of the McGill filter. Though it is hard to get MFP pairs to measure jitter using Butterworth filtered data, the jitter value results are close to McGill filtered data results. The ability to measure jitter and the measurement accuracy were quantitatively evaluated using synthetic MUPTs and four simulated EMG signals with various expected jitter values. In general, the measurement results are close to the expected jitter values, the measurement errors are acceptable, and can reflect individual neuromuscular jitter information.

The measurement error mainly results from the effect of noise. In particular, if a MFP pair is composed of a large MFP and a relatively small one (close to the detection threshold), the noise level may be relatively high and the small MFP contributions may be covered by noise so that occurrence times of the corresponding contributions are changed or even missed. Similarly, large measurement errors and false or missed blockings may appear. In addition, errors of interpolation can also contribute to measurement errors, and overlap of individual MFPs can cause specific near MFP contributions to be missed so that some false blockings may be identified.

To assure the accuracy of jitter measurements, IPIs should be above 400 μs in each MFP pair. Because neuromuscular jitter is usually measured in about 20 fibre pairs in each muscle investigated it is very convenient and advantageous to measure jitter using

CN MUPs. Using the McGill filter gave good time resolution and it is more computational efficient than the Acceleration filter. The more efficient use of the MST algorithm will shorten jitter measurement time so it will be more practical in clinical use and may be able to provide more real data to further improve the method.

Chapter 5 Conclusions and Recommendations

Based on the results from simulated EMG signals presented in the previous chapter, the automated jitter measurement algorithm has good performance and can correctly represent individual neuromuscular jitter information. By analysing MUP acceleration, choosing suitable filters and choosing suitable acceleration thresholds, near MFP contributions can be detected. This was tested for both SF and CN signals. In addition, by constantly detecting significant MFP contributions in MUP trains, MFP pairs can be chosen to calculate neuromuscular jitter. Instead of the traditional way of manually choosing MUPs for jitter calculation, all the process steps are automated with adaptive algorithms and thresholds. To automatically isolate MUPs in a MUPT, nearest neighbour clustering and minimum spanning tree algorithms were used. With the set of the available filtered MUPs individual MFP contributions could be identified and specific MFP pairs could be selected for jitter calculation.

One limitation for the method is the temporal overlap of MFPs, these results show 300 μs is the minimum time resolution required and with more than 400us better results are expected. Due to superposition of MFPs, some near MFP contributions may be missed so that the detection scheme will underestimate the true number of the contributions to a certain extent. However, the missed contributions usually do not affect the measurement of neuromuscular jitter.

The proposed algorithm can consistently measure jitter in a variety of EMG signals. Because measuring jitter using CN MUPs can acquire more individual MFP pairs than using SF EMG from fewer EMG signals, it could be adapted to a real clinic setting.

Further improvements and evaluation of the performance of the measurement algorithm is needed when trying to apply it to real EMG signal analysis. By comparing the measurement results from CN MUPs with SF MUPs for similar real subjects, parameters for thresholds should be adjusted to get more accurate results.

Bibliography

[1] Basmajian JV, DeLuca CJ: *Muscles Alive: Their Functions Revealed by Electromyography (5th edition)*. Williams and Wilkins, Baltimore, MD. USA, 1985.

[2] Antoni L, Stalberg E, Sanders D: Automated analysis of neuromuscular 'jitter'. *Computer Programs in Biomedicine* 1983; 16: 175-188.

[3] Brown WF: *The Physiological and Technical Basis of Electromyography*. Butterworth Publishers, Stoneham, MA. USA, 1984.

[4] Paoli GM: *Estimating Certainty in Classification of Motor Unit Action Potentials*. Master's thesis, University of Waterloo, Waterloo, Ont. Canada, 1993.

[5] Dumitru D: Physiologic basis of potentials recorded in electromyography. *Muscle Nerve*, 2000; 23: 1667-1685.

[6] Stashuk DW, Doherty TJ: *The normal motor unit action potential*. (Notes, inner communication 1997).

[7] King JC, Dumitru D, Nandedkar S: Concentric and single fiber electrode spatial recording characteristics. *Muscle Nerve* 1997; 20.

[8] Sheng Ma, Measuring neuromuscular jitter in motor unit potentials. Master's thesis, University of Waterloo, Ontario Canada 2003.

[9] Nandedkar SD, Stalberg E: Simulation of single muscle fibre action potentials. *Medical & Biological Engineering & computing* 1983; 21: 158-165.

[10] Stashuk DW. EMG signal decomposition: how can it be accomplished and used? *Journal of Electromyography and Kinesiology*, 2001; 11: 151-173.

[11] Stashuk DW, Brown WF: *Quantitative electromyography*. (Notes, inner communication).

[12] Stalberg E, Soono M: Assesment of variability in the shape of the motor unit action potential

[13] Thiele B, Stalberg E: The bimodal jitter: a single fibre electromyographic finding. *Journal of Neurology, Neurosurgery, and Psychiatry* 1974; 37: 403-411.

[14] Nandedkar SD, Sanders DB, Stalberg EV, Andreassen S: Simulation of concentric needle EMG motor unit action potentials. *Muscle Nerve* 1988; 11 151-159.

[15] Stashuk DW: Decomposition and quantitative analysis of clinical electromyographic signals. *Medical Engineering & Physics*, 1999; 21: 389-404.

[16] Ekstedt J, Stalberg E: Single fibre electromyography for the study of the microphysiology of the human muscle. *New Developments in Electromyography and Clinical Neurophysiology*, vol. 1: 89-112 (Karger, Basel 1973).

[17] Stalberg E, Ekstedt J: Single fibre EMG and microphysiology of the motor unit in normal and diseased human muscle. *New Developments in Electromyography and Clinical Neurophysiology*, vol. 1: 113-129 (Karger, Basel 1973)

[18] Stashuk DW: Detecting single fiber contributions to motor unit action potentials. *Muscle Nerve*, 1999; 22: 218-229.

[19] Gath I, Stalberg EV: Techniques for improving the selectivity of electromyographic recordings. *IEEE Transactions on Biomedical Engineering* 1976; 23: 467-472.

[20] Sanders DB, Stalberg E: AAEM Minimonograph #25: single-fiber electromyography. *Muscle Nerve* 1996; 19: 1069-1083.

[21] Stalberg E, Ekstedt J, Broman A: The electromyographic jitter in normal human muscles. *Electroencephalography and Clinical Neurophysiology* 1971; 31: 429-438.

[22] Trontelj JV, Mihelin M, Fernandez JM, Stalberg E: Axonal stimulation for end-plate jitter studies. *Journal of Neurology, Neurosurgery, and Psychiatry* 1986; 49: 677-685.

[23] Ekstedt J, Nilsson G, Stalberg E: Calculation of the electromyographic jitter. *Journal of Neurology, Neurosurgery, and Psychiatry* 1974; 37: 526-539.

[24] Gilchrist JM, ad hoc Committee: Single fiber EMG reference values: a collaborative effort. *Muscle Nerve* 1992; 15: 151-161

[25] Ertas M, Baslo MB, Yildiz N, Yazici J, Oge AE: Concentric needle electrode for neuromuscular jitter analysis. *Muscle Nerve* 2000; 23: 715-719.

[26] Buchman AS, Garratt M: Determining neuromuscular jitter using a monopolar electrode. *Muscle Nerve* 1992; 15: 615-619.

[27] Stashuk DW: Simulation of electromyographic signals. *Journal of Electromyography and Kinesiology*, 1993; 3: 157-173.

[28] Lindstrom L, Petersen I: Power spectrum analysis of EMG signals and its applications. *Computer-Aided Electromyography*, vol. 10: 1-51 Editor: Desmedt JE; (Karger, Basel 1983).

[29] Rabiner LR, Gold B: *Theory and application of digital signal processing*. Prentice-hall, Englewood Cliffs, NJ. USA, 1975.

[30] Porat B: *A course in digital signal processing*. John Wiley & Sons, New York, USA, 1997.

[31] Usui S, Amidror I: Digital low-pass differentiation for biological signal processing. *IEEE Transactions on Biomedical Engineering* 1982; 29: 686-693.

[32] McGill KC, Cummins KL, Dorfman LJ: Automatic decomposition of the clinical electromyogram. *IEEE Transactions on Biomedical Engineering* 1985; 32: 470-477.

[33] David Randall, Warren Burggren, and Kathleen French. *Eckert Animal Physiology,* chapter Muscles and Animal Movement , Figure 10-1, page 352. W. H. Freeman and Company, 4th edition, 1998.

[34] Andrew Hamilton-Wright, Daniel W. Stashuk. Physiologically Based Simulation of Clinical EMG Signals. IEEE Transactions on biomedical engineering, Vol.52 No.2 Feb. 2005